

LOW TEMPERATURE PHOTOLUMINESCENCE STUDY IN GaS-GaSe LAYERED
CRYSTALS

A THESIS SUBMITTED TO
THE GRADUATE SCHOOL OF NATURAL AND APPLIED SCIENCES
OF
THE MIDDLE EAST TECHNICAL UNIVERSITY

119 139
BY

KADİR GÖKŞEN

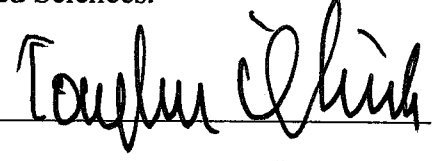
119139

**T.C. YÜKSEKÖĞRETİM KURULU
DOKÜMANTASYON MERKEZİ**

IN PARTIAL FULFILLMENT OF THE REQUIREMENTS FOR THE DEGREE OF
MASTER OF SCIENCE
IN
THE DEPARTMENT OF PHYSICS

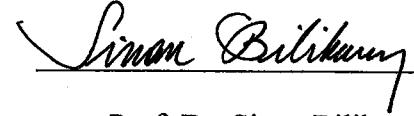
AUGUST 2002

Approval of the Graduate School Natural and Applied Sciences.



Prof. Dr. Tayfur Öztürk
Director

I certify that this thesis satisfies all the requirements as a thesis for the degree of Master of Science.



Prof. Dr. Sinan Bilikmen
Head of Department

This is to certify that we have read this thesis and that in our opinion it is fully adequate, in scope and quality, as a thesis for the degree of Master of Science.



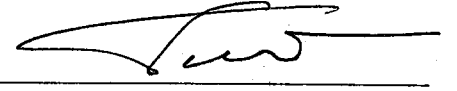
Prof. Dr. Hüsnü Özkan
Co-supervisor



Prof. Dr. Nizami Hasanli
Supervisor

Examining Committee Member

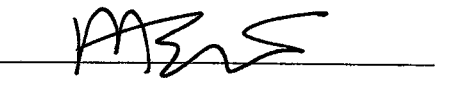
Prof. Dr. Nizami Hasanli



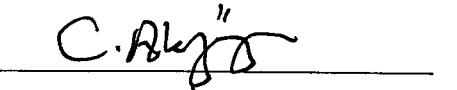
Prof. Dr. Hüsnü Özkan



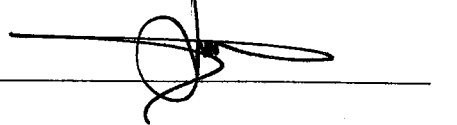
Prof. Dr. Raşit Turan



Prof. Dr. Yakup Cevdet Akgöz



Assoc. Prof. Dr. Mehmet Parlak



ABSTRACT

LOW TEMPERATURE PHOTOLUMINESCENCE STUDY IN GaS-GaSe LAYERED CRYSTALS

Gökşen, Kadir

M. S. Department of Physics

Supervisor: Prof. Dr. Nizami Hasanli

Co-supervisor: Prof. Dr. Hüsnü Özkan

August 2002, 73 pages

The impurity states in $\text{GaS}_x\text{Se}_{1-x}$ single crystals were studied for the values of $x = 1, 0.5$ and 0 by photoluminescence experiments. For each value of compositional parameter, x , (for GaS, $\text{GaS}_{0.5}\text{Se}_{0.5}$ and GaSe crystals), the variation of the photoluminescence spectra as a function of temperature and excitation laser intensity was investigated. As a result of analysis, the energy band diagram for each crystal was drawn.

Keywords: Photoluminescence, impurity states, recombination mechanisms, band structure

ÖZ

GaS-GaSe KATMANLI KRİSTALLERİNİN DÜŞÜK SICAKLIKTA FOTOIŞIMA İNCELEMESİ

Gökşen, Kadir

Yüksek Lisans, Fizik Bölümü

Tez Yöneticisi: Prof. Dr. Nizami Hasanli

Ortak Tez Yöneticisi: Prof. Dr. Hüsnü Özkan

Ağustos 2002, 73 sayfa

GaS_xSe_{1-x} katlı kristallerinin safsızlık durumları, $x = 1, 0.5$ ve 0 değerleri için fotoışımaya deneyleri aracılığıyla incelendi. Bileşik parametresinin (x) her bir değeri için (GaS, GaS_{0.5}Se_{0.5} ve GaSe kristalleri için), fotoışımaya spektrumunun sıcaklığa ve lazer uyarma şiddetine bağımlılığı incelendi. Analizler sonucu, her bir kristal için enerji bandı diyagramı çizildi.

Anahtar kelimeler: Fotoışımaya, safsızlık durumları, yeniden birleşme mekanizmaları, band yapısı

ACKNOWLEDGMENTS

I would like to thank Prof. Dr. Nizami Hasanli for his complete encouragement and continuous support to this study. Since the beginning of this work, Prof. Hasanli helped whenever I need with his valuable guidance and friendly attitude. For this study, I owe him more than I can express. I also want to thank Prof. Dr. Hüsnu Özkan for his valuable helps.

At the same time, I would like to thank Prof. Dr. Atilla Aydınli, a real experimental physicist, from Bilkent University. He helped me with patience whenever I need, from the initial stages of this work to the final. I learned a lot about optical spectroscopy with him. I also thank Coşkun Kocabaş, especially for his great efforts in the beginning of the experimental work and in fitting process.

Finally, I would like to thank my family and all of my friends, who always supported me with their uninterrupted love and patience.

To speak the truth, I owe all the people I mentioned a lot and, in fact, they share my successes.

TABLE OF CONTENTS

ABSTRACT	iii
ÖZ	iv
ACKNOWLEDGMENTS	v
TABLE OF CONTENTS	vi
LIST OF FIGURES	viii
CHAPTER	
1. INTRODUCTION	1
2. THEORETICAL APPROACH	5
2.1 Introduction	5
2.2 Impurity States in Compound Semiconductors	5
2.3 Crystal Symmetry	6
2.4 Optical Properties of Semiconductors	8
2.4.1 Photoluminescence	8
2.4.2 Recombination Mechanisms.....	9
2.4.2.a Band-to-Band Transitions	9
2.4.2.b Free-to-Bound Transitions	11
2.4.2.c Free and Bound Exciton Emissions	12
2.4.2.d Donor-Acceptor Pair Transitions	12

2.4.3	Dependence of Photoluminescence of Semiconductors on Laser Excitation Power	13
2.4.4	Dependence of the Peak Energy of the Donor-Acceptor Pair Photoluminescence Band on Excitation Intensity	18
3.	EXPERIMENTAL SETUP AND TECHNIQUES USED IN PL EXPERIMENTS	25
3.1	Experimental Setup Used in Photoluminescence Experiments	25
3.2	Experimental Techniques Used in Photoluminescence Experiments	26
4.	RESULTS AND DISCUSSION	28
4.1	Introduction	28
4.2	Results and Discussion of the PL Experiment for GaS crystal	28
4.2.1	Experimental Details	28
4.2.2	Results and Discussion	29
4.2.3	Conclusions	44
4.3	Results and Discussion of the PL Experiment for GaS _{0.5} Se _{0.5} crystal	45
4.3.1	Experimental Details	45
4.3.2	Results and Discussion	45
4.3.3	Conclusions	53
4.4	Results and Discussion of the PL Experiment for GaSe crystal	54
4.4.1	Experimental Details	54
4.4.2	Results and Discussion	55
4.4.3	Conclusions	65
5.	CONCLUSIONS	67
	REFERENCES	70

LIST OF FIGURES

FIGURES

2.1	Stacking sequences for the ϵ - and β -polytypes of GaS and GaSe.....	7
2.2	Radiative and nonradiative transition in PL by excitation and recombination.....	10
2.3.a	Donor-acceptor transition.....	14
2.3.b	Effect of Coulomb interaction on emission energy.....	14
3.1	Schematic diagram of photoluminescence setup used in experiments.....	25
3.2	Deconvolution of the photoluminescence spectra into two Gaussian lineshapes..	27
4.1	Temperature dependence of PL spectra from GaS single crystal in the 525–860 nm range.....	30
4.2	Temperature dependence of the peak intensity of A, B, and C bands The arrows show the starting points of the intensive quenching.....	32
4.3	Temperature dependence of the peak energy of bands A, B, and C.....	34
4.4	Linewidths of the A, B, and C bands as a function of the square root of temperature.....	36
4.5	Excitation intensity dependence of the photoluminescence spectra of GaS at $T = 9$ K.....	37
4.6	Excitation intensity dependence of the peak photoluminescence intensity of bands A, B, and C in GaS crystals.....	39
4.7	Proposed model for the donor–acceptor pair recombination processes in GaS at $T = 9$ K.....	43
4.8	PL spectra of $\text{GaS}_{0.5}\text{Se}_{0.5}$ in the temperature range of 15–170 K.....	47

4.9	Temperature dependencies of the E_g , A- and B-bands peak energies for $\text{GaS}_{0.5}\text{Se}_{0.5}$	48
4.10	Photoluminescence intensity of A- and B-bands at the maximum of the emission intensity as a function of reciprocal temperature, the arrows at 50 and 90 K show the starting points of intensive quenching.....	49
4.11	Dependencies of the photoluminescence intensity at the A- and B-bands maximum versus excitation laser intensity at $T = 15$ K.....	51
4.11	Proposed energy band diagram for the observed deep level luminescence in $\text{GaS}_{0.5}\text{Se}_{0.5}$ at $T = 15$ K.....	52
4.13	PL spectra of undoped p-type GaSe as a function of temperature.....	56
4.14	Temperature dependences of GaSe PL intensity at the emission band maxima, the arrows at 35 and 90 K show the starting points of the intensive quenching of the A and B bands respectively.....	58
4.15	Excitation laser intensity versus GaSe emission B-band peak energy at 10 K.....	60
4.16	Dependence of GaSe PL intensity at the emission band maxima vs. excitation laser intensity at 10K.....	62
4.17	Proposed energy band diagram for the observed deep level luminescence in GaSe at $T = 10$ K.....	64

CHAPTER 1

INTRODUCTION

Many kinds of luminescence emission were observed from lightning, aurora, fireflies and a certain sea bacteria long before there were written records. Luminescence of solids was reportedly first observed in 1603 by Cascarilio, who heated some powdered natural barium sulphate with coal and found that the cooled porous cake glowed at night. After that, in 1888, German physicist Wiedemann introduced the term *luminescence* corresponding to fluorescence and phosphorescence, which were only known types of luminescence then. Wiedemann defined luminescence as denoting “all those phenomena of light which are not caused solely by an increase in temperature”. Today luminescence is considered to be a process by which a material generates non-thermal radiation that is *characteristic of the particular material*. In addition to the great variety of luminescence emissions from different materials, there is variety in the kinds of the input energies that can excite luminescent materials. Over the years, it has become customary to use prefixes to distinguish between the different causes of excitation like photoluminescence, bioluminescence, electroluminescence etc., which will be explained later in detail in theoretical part.

A wide variety of binary and ternary layered semiconductors attract much interest due to possible optoelectronic applications from ultraviolet to the infrared [1-3]. For the

most part, optoelectronic properties of these materials are dominated by defects of various types and the interactions between them. In spite of the significant experimental and theoretical efforts devoted to the study of these materials, both experimental data and the overall theoretical understanding of them lacks a coherent and complete framework. In fact, even in binary compounds, little work has been done both experimentally and theoretically.

Photoluminescence (PL) spectroscopy is a very suitable and widely used technique to study the defect structures of semiconductors. Unfortunately, most of the work on layered semiconductors has concentrated on the near band edge emission of these materials. Only a little amount of data exists on shallow and deep PL bands with emission energies below the band gaps of these semiconductors.

GaS and GaSe crystals both belong to a family of semiconductors of the $A^{III}B^{VI}$ -type which crystallize in a layered structure with layers containing four monoatomic sheets in the order of S-Ga-Ga-S or Se-Ga-Ga-Se respectively. In both types of crystals and their mixture GaS_xSe_{1-x} , interlayer interactions are dominated by van der Waals forces while intralayer-bonding forces are primarily ionic-covalent in nature. Due to weak interlayer interaction, all GaS, GaSe and GaS_xSe_{1-x} crystals can be cleaved along these layers. Depending on period of stacking sequences, GaSe crystallizes in ϵ , β , γ and δ modifications while GaS only crystallizes in β modification. However, when we come to GaS_xSe_{1-x} crystals, the crystal structure is dependent on the value of x . GaS has an indirect band gap about 2.59 eV at 300 K [4] and a direct band gap about 3.04 eV, while GaSe has an indirect band gap about 2.102 eV and a direct band gap about 2.127 eV at 4 K [5]. But, GaS_xSe_{1-x} mixed crystals have a range of band gap energy values, again,

depending on the value of x , as expected (e.g. GaS_{0.5}Se_{0.5} crystal has an indirect band gap of 2.27 and 2.334 eV at 300 and 15 K respectively) [5-7].

For the value of its band gap energy, GaS is considered to be a promising material for near-blue light emitting devices. GaS exhibits PL in the green-blue region [8-10]. PL of both Zn doped and undoped GaS has been investigated by several authors [11,12]. Near band edge luminescence attributed to recombination of shallow donors with distant acceptors has been proposed [5]. Deep level luminescence for GaS at 77 K was also observed [13]. However there are no PL data below 77 K and no detailed analysis of deep level luminescence spectra of GaS in the literature to our knowledge.

For GaSe, we can say that a considerable work has been carried out on the photoluminescence from GaSe. The low-temperature PL spectrum of GaSe is quite complex and shows a large number of sharp lines near the band edge and wider bands away from the band edge. Band-edge luminescence in GaSe is very rich in the number of lines observed. This is because, in GaSe, the indirect minimum of the conduction band is 25 meV lower than the direct minimum. As a result of this, photoexcited carriers populate both bands and give rise to many lines owing to radiative recombination related to these bands. Both direct and indirect free and bound excitonic structures are observed [14,15]. Wide bands observed at lower energies are attributed to intrinsic defects in the case of undoped samples and to impurities and defects for doped samples. For undoped ϵ -GaSe [16], it has been shown that increasing concentration of defects leads to increasing PL intensity as well as a blue shift of the band. PL spectra of undoped samples have been used to compare with the PL spectra of Tm-doped GaSe and three bands at 590, 610 and 690 nm have been observed in undoped GaSe [17]. Both excitonic

and impurity-related emission lines have been observed in GaSe at 4.2 K in the range 580-610 nm [18]. No recombination radiation specific to the introduced dopant had been detected. Donor and acceptor states taking place in the recombination were thought to have originated from structural defects whose concentration increased with increasing impurity content. PL from both undoped and Cu-doped GaSe at 80 K have been studied [15] and donor states related to structural defects as well as acceptor states related to Cu have been proposed. Several PL studies involving various impurities such as Cd [19], Ag [20], Mn [21], Zn [22], Cu, Zn, Cd, Sn, and I [23] have also revealed both excitonic and impurity-related lines in GaSe. In spite of all these data, PL spectra of undoped GaSe away from the excitonic region are not well characterized at low temperatures ($T < 77$ K). In particular, no systematic analysis of the defect related PL spectra of undoped GaSe exists in the literature to our knowledge.

For $\text{GaS}_x\text{Se}_{1-x}$, we can also say that not much work has been carried out on PL study of these mixed crystals. Long-wavelength optical phonons in $\text{GaS}_x\text{Se}_{1-x}$ layered mixed crystals were studied by infrared (IR) reflection and Raman scattering experiments [24-27]. Near band edge luminescence from a series of $\text{GaS}_x\text{Se}_{1-x}$ mixed crystals have also been measured at 4.2 K and attributed to recombination on shallow donor and acceptor states ($E_A = E_D = 25$ meV). They were thought to be due to structural defects [5]. However, there is no data on the temperature and excitation intensity dependence of PL spectra in $\text{GaS}_x\text{Se}_{1-x}$ crystals in the literature to our knowledge.

CHAPTER 2

THEORETICAL APPROACH

2.1 Introduction

In this chapter we will deal with the basic information needed to analyze impurity states in semiconductors and theoretical considerations used for optical characterization of GaS-GaSe crystal system.

2.2 Impurity States in Compound Semiconductors

Impurities play very important role in semiconductors because it is the presence of impurity atoms that largely determine the practical applications of semiconductors [28]. A well known fact, the use of gold to give fast recombination in silicon junctions that require nanosecond switching times, also proves the importance of impurity atoms in semiconductors [29]. When an impurity atom is introduced in a lattice, it faces with several types of interactions. The impurity is called as a donor, if it replaces one of the constituent atoms of the crystal and provides crystal with one or more additional electrons than the atom it replaces. The excess electron or electrons have weak bounds. The impurity is called as an acceptor, if it replaces one of the constituent atoms of the crystal and supplies less electrons than the atom it replaces. A missing electron due to

impurity is considered as a hole. A hole or holes have also weak bounds and behave as the localized state. Te atoms on As-site of GaAs crystal can be an example of a donor and Zn atoms on Ga-site of GaAs crystal can be an example of an acceptor.

The impurities do not always replace constituent atoms of the crystal but sometimes they may locate themselves in an interstitial position, which causes another type of impurity. In such a case, the outer-shell electrons of this impurity are available for conduction, and for this reason the impurity is always considered as a donor. Besides this, a missing atom in the crystal structure may also act like an impurity. If this missing atom deprives the crystal of one or more electrons, then it is considered as an acceptor. Interstitial impurities and vacancies generally combine to form a molecular impurity that may be either donor because of interstitial impurities or an acceptor because of vacancies.

2.3 Crystal Symmetry

The layer compounds GaSe and GaS form a continuous series of $\text{GaS}_x\text{Se}_{1-x}$ mixed crystals in the whole range of compositional parameter ($0 \leq x \leq 1$) [30]. They all crystallize in hexagonal unit cell structure. Their structure, however, are not all the same throughout the whole range of x , which means that there are some stacking differences. There are four basic structures, called as polytypes, depending on period of stacking sequences, named as ϵ , β , δ and γ . GaSe crystals grown from the melt by the Bridgman method present ϵ modification whereas GaS crystals invariably present β modification, which sometimes is also found in vapor-grown GaSe. At $x = 0.5$ the $\text{GaS}_x\text{Se}_{1-x}$ crystal is a mixture of the ϵ - and β -polytypes. In our experiments, studied

crystals had three different value for the compositional parameter x , which are 1, 0.5 and 0. Further, we will deal only with the structure of related polytypes to our experiments which are ϵ and β polytypes.

In both ϵ and β polytype structures, the unit cells span two layers of crystal and contains 8 atoms. The difference between ϵ and β polytype structures are only the stacking of atoms in the crystal structure. This difference can be understood more easily by looking at the Fig. 2.1 below more easily. In this figure, two different views are given for convenience. Fig. 2.1 shows clearly the structure of both polytypes and the differences between them.

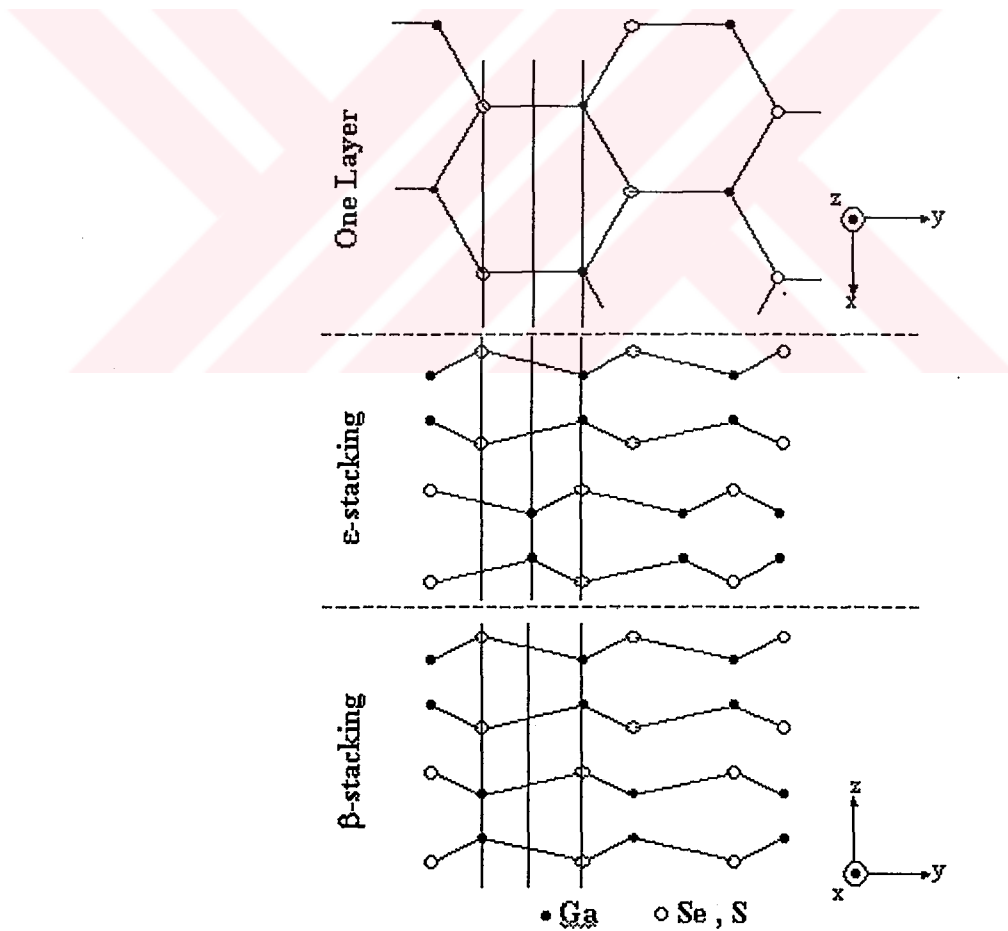


Fig. 2.1 Stacking sequences for the ϵ - and β -polytypes of GaS and GaSe

2.4 Optical Properties of a Semiconductor

2.4.1 Photoluminescence

Photoluminescence spectroscopy is a contactless, nondestructive method of probing the electronic structure of materials. When a semiconductor is energized by some external means, it emits radiation. Light is directed onto a sample, where it is absorbed and imparts excess energy into the material in a process called "photo-excitation." One way this excess energy can be dissipated by the sample is through the emission of light. This process is called as luminescence. There are several ways to excite the sample to cause luminescence. One possible way is to excite the sample by applying an external current, called as electroluminescence. Another way is production of radiation from sample by heating it, called as thermoluminescence, or doing the same thing by electron bombardment is called as cathodoluminescence. But the most common method is by absorption of photons of energy higher than the band gap energy, the resulting process in which photons of energy lower than the excitation photons are radiated is called as photoluminescence. The intensity and spectral content of photoluminescence is a direct measure of various important material properties.

Specifically, photo-excitation causes electrons within the material to move into permissible excited states. When these electrons return to their equilibrium states, the excess energy is released and may include the emission of light (a radiative process) or may not (a nonradiative process). The energy of the emitted light or photoluminescence is related to the difference in energy levels between the two electron states involved in the transition that is, between the excited state and the equilibrium state. The quantity of the emitted light is related to the relative contribution of the radiative process.

Thus, in a photoluminescence experiment, firstly electron-hole pairs are excited (Fig. 2.2,A). Then before they recombine radiatively, they reach a quasi-thermal equilibrium among themselves which lasts much shorter than the recombination process. Thus a photoluminescence process involves three steps [31]:

a-) Excitation: Electron-hole pairs are excited by an external energy source

b-) Thermalization: Excited pairs relax towards quasi-thermal equilibrium distributions.

c-) Recombination: Thermalized pairs recombine radiatively to produce emission.

2.4.2 Recombination Mechanisms

Three types of optical transitions may take place in a semiconductor when it is energized by some external means. These are band-to-band transitions, free-to-bound transitions and donor-acceptor pair transitions.

2.4.2.a Band-to-Band Transitions

These types of transitions, involving free holes and free electrons, are sometimes called free-to-free transitions. In a perfect semiconductor e-h pairs will thermalize and accumulate at the conduction band and valence band extrema where they tend to recombine. The rate of emission is given by the equation

$$R = n_i n_f P , \quad (2.1)$$

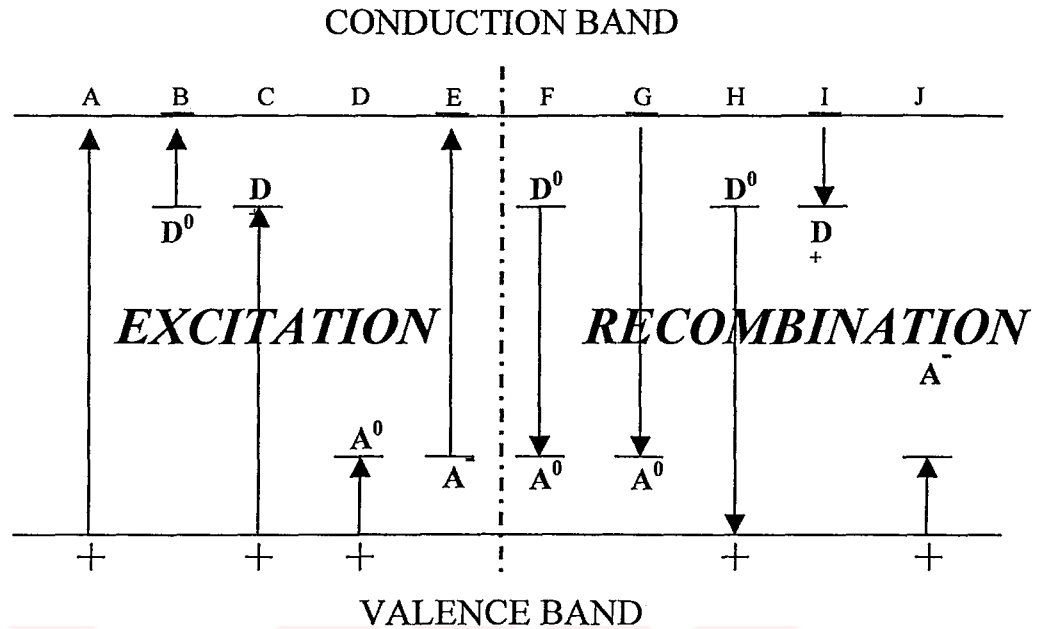


Fig. 2.2 Radiative and nonradiative transition in PL by excitation and recombination

where n_i and n_f are the initial and final densities of states, and P is the probability that 1 carrier/cm² at the higher energy will make a radiative transition into 1 vacancy/cm² in the lower state and can be calculated by using quantum mechanical principles related to photon-electron interactions. This probability is proportional to the absorption coefficient.

In a semiconductor having a direct band gap, the recombination of electron-hole pairs occurs radiatively with a high probability. So in such a semiconductor, like GaAs, recombination transition is vertical and radiated photon energy is given by the equation:

$$h\nu = E_f - E_i, \quad (2.2)$$

where E_f and E_i are the final and initial state energies, respectively. In indirect band gap semiconductors, like Si and Ge, electron-hole pairs can recombine via phonon assisted transitions, and the emitted photon has the energy given by the equation:

$$h\nu = E_f - E_i \pm h\Omega, \quad (2.3)$$

where $h\Omega$ is the energy of phonon and the + and – signs correspond to phonon emission or absorption, respectively. As easily seen from above formula, phonon emission can shift the band-to-band spectrum to lower energies. This above process is called band-to-band transition.

2.4.2.b Free-to-Bound Transitions

Band-to-band transitions dominate at high temperatures where all impurities are ionized but at low temperatures the carriers become frozen on impurities. As an example, we can consider a p -type sample which contains N_A acceptors per unit volume. If we do a PL experiment on this sample, we see that at low photoexcitation the density of free electrons forming in the conduction band is much smaller than N_A . These electrons can recombine with the holes trapped on the acceptors radiatively or nonradiatively (Fig. 2.2,G). Transitions like this which involves a free carrier (an electron in our case) and a charge which is bound to an impurity (a hole in our case) are called as free-to-bound transitions. In such transitions, the energy of the emitted photon is given by $E_G - E_A$, where E_A is the acceptor binding energy.

2.4.2.c Free and Bound Exciton Emissions

In photoluminescence experiments, on high purity and high quality semiconductors at low temperatures, it is expected that photoexcited electrons and holes are attracted to each other by Coulomb interaction and form excitons. As a result, the emission spectra should be dominated by radiative annihilation of excitons producing the so-called free-exciton peak. When the sample contains a small number of impurities in their neutral state, which is a common occurrence at low temperatures, the excitons will be attracted to these impurities via van der Waals interaction. Since the attraction decreases the exciton binding energy, neutral impurities are very efficient at trapping excitons to form bound excitons at low temperature.

2.4.2.d Donor-Acceptor Pair Transitions

Semiconductors quite often contain both donors and acceptors. In such semiconductors, under equilibrium conditions, some of the electrons from donors are captured (or compensated) by the acceptors. For this reason, such semiconductors are called as compensated. They contain both ionized donors (D^+) and acceptors (A^-). Electrons and holes can be formed in the conduction and valence bands respectively, by optical excitation (Fig. 2.2, A). Then these carriers can be trapped at D^+ and A^- sites and they produce neutral donors (D^0) and acceptors (A^0). In returning the equilibrium, some of the electrons on neutral donors will recombine radiatively with the holes on the neutral acceptors (Fig 2.2, F). Such a process is called as donor-acceptor pair transition (DAP). This transition can be represented by

$$D^0 + A^0 = h\nu + D^+ + A^-, \quad (2.4)$$

The photon emitted in such a transition has the energy

$$h\nu_\infty = E_G - E_D - E_A, \quad (2.5)$$

where E_G is the band gap energy of the sample, E_D is the binding energy of the donors and E_A is the binding energy of the acceptors as isolated impurities. But in this equation, we see that the Coulomb interaction between ionized donors and acceptors is neglected.

So taking into account the Coulomb interaction, our equation becomes

$$h\nu = E_G - E_D - E_A + q^2/(\epsilon r), \quad (2.6)$$

where ϵ is the static dielectric constant and r is the distance between ionized donor and acceptor (Fig. 2.3).

2.4.3 Dependence of Photoluminescence of Semiconductors on Laser Excitation Power

As the power of the excitation light source is changed, the variation of photoluminescence intensity depending on this power can be used to identify the underlying recombination process [32]. It has also been found that the luminescence

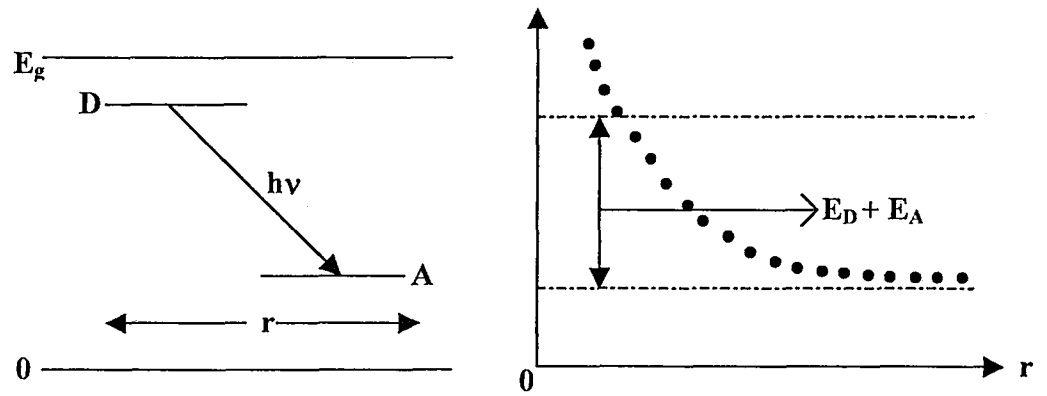


Fig. 2.3 a-)Donor-acceptor transition, b-)Effect of Coulomb interaction on emission energy

intensity I of the near band edge photoluminescence emission lines is proportional to L^k , which can be expressed as

$$I \propto L^k \quad (2.7)$$

where L is the power of the exciting laser radiation [33 - 36]. For exciton like transitions, k has the value between 1 and 2 ($1 < k < 2$) and for free-to-bound and donor-acceptor pair transitions ($D^0 A^0$), k has a value smaller than 1 ($k < 1$) [37].

A model for excitation power dependence of photoluminescence was proposed by T. Schmidt *et al* [37] to explain the features of photoluminescence observed in the experiment. While proposing this model, they took into account all the transitions shown in Fig. 2.2. In other words, they assumed that photoexcited electron-hole pairs can recombine by the following transitions: free-exciton recombination, radiative recombination of donor- and acceptor-bound excitons, donor-acceptor pair recombination, radiative recombination of a free electron and a neutral acceptor, radiative recombination of a free hole and a neutral donor, and nonradiative transitions

of free electrons and holes to ionized donors and acceptors respectively. They also assumed that, for convenience, the electron concentration in the conduction band, n , is equal to the concentration of holes in the valence band, p . If the thermal dissociation of free and bound excitons is also neglected, all transitions mentioned above can be described by the following set of coupled differential equations:

$$\frac{dn}{dt} = iL - an^2 - gn(N_D - N_D^0) - enN_A^0 \quad (2.8)$$

$$\frac{dn_{FE}}{dt} = a n^2 + jL - \left[\frac{1}{\tau_{FE}} + \frac{1}{\tau_{FE}^{nr}} \right] n_{FE} - b n_{FE} N_D^0 - c n_{FE} N_A^0 \quad (2.9)$$

$$\frac{dn_{DX}}{dt} = b n_{FE} N_D^0 - \left[\frac{1}{\tau_{DX}} + \frac{1}{\tau_{DX}^{nr}} \right] n_{DX} \quad (2.10)$$

$$\frac{dn_{AX}}{dt} = c n_{FE} N_A^0 - \left[\frac{1}{\tau_{AX}} + \frac{1}{\tau_{AX}^{nr}} \right] n_{AX} \quad (2.11)$$

$$\begin{aligned} \frac{dN_{A^0}}{dt} = & h(N_A - N_A^0)n + i(N_A - N_A^0)L - c n_{FE} N_A^0 \\ & + \left[\frac{1}{\tau_{AX}} + \frac{1}{\tau_{AX}^{nr}} \right] n_{AX} - d N_D^0 N_A^0 \quad (2.12) \end{aligned}$$

$$\begin{aligned} \frac{dN_{D^0}}{dt} = & g(N_D - N_{D^0})n + kN_{D^0}L - b n_{FE}N_{D^0} \\ & + \left[\frac{1}{\tau_{DX}} + \frac{1}{\tau_{DX}^{nr}} \right] n_{DX} - dN_{D^0}N_{A^0} - fN_{D^0}n \end{aligned} \quad (2.13)$$

In above equations, N_D and N_A are the concentrations of donors and acceptors, N_{D^0} and N_{A^0} are the concentrations of neutral donors and acceptors, τ_{FE} and τ_{FE}^{nr} are the radiative and nonradiative lifetimes of donor and acceptor bound excitons, and τ_{DX} , τ_{DX}^{nr} , τ_{AX} , τ_{AX}^{nr} are the radiative and nonradiative lifetimes of donor and acceptor bound excitons, respectively. n_{FE} , n_{DX} and n_{AX} are the concentrations of free and bound excitons, respectively and L is the laser excitation intensity. The coefficients a, b, \dots, l are the transition rates of the processes mentioned above in Fig. (2.2). The charge neutrality was fulfilled by assuming $n = p$. For simplicity, phonon replica, two electron and two hole transitions, and the recombination of excitons bound to ionized donors ($D^+ X$) were also neglected because these are weak transitions. The term j in Eqn. (2.9) describes the direct formation of free excitons and can be neglected for laser light energies, $h\nu$, exceeding the band gap energy, E_g .

For constant N_{D^0} and N_{A^0} , assuming that only a small portion of the free electron hole pairs form excitons and photoexcited carriers recombine via defect states of donors and acceptors and neglecting the term an^2 in Eqn. (2.8), in the steady state, we get from Eqn. (2.9) and (2.11) the luminescence intensities of free and bound excitons, I_{FE} , I_{DX}^0 and I_{AX}^0 as follows:

$$I_{FE} = \frac{n_{FE}}{\tau_{FE}} = \frac{\beta}{\tau_{FE}} n^2 \quad (2.14)$$

$$I_{D^0 X} = \frac{n_{DX}}{\tau_{DX}} = \frac{bN_{D^0}\beta}{1 + \frac{\tau_{DX}}{\tau_{DX}^{nr}}} n^2 \quad (2.15)$$

$$I_{A^0 X} = \frac{n_{DA}}{\tau_{AX}} = \frac{cN_{A^0}\beta}{1 + \frac{\tau_{AX}}{\tau_{AX}^{nr}}} n^2 \quad (2.16)$$

$$\beta = \frac{a}{\left[\frac{1}{\tau_{FE}} + \frac{1}{\tau_{FE}^{nr}} \right] + bN_{D^0} + cN_{A^0}} \quad (2.17)$$

Assuming the intensity of free-to-bound transitions to be proportional to the respective transition rates, we can write

$$I_{hD^0} \sim nN_{D^0} \quad (2.18)$$

$$I_{eA^0} \sim nN_{A^0} \quad (2.19)$$

For variation of N_{D^0} and N_{A^0} with L , assuming $I_{D^0 A^0}$ is proportional to $N_{D^0}N_{A^0}$, they

obtained the following relation for donor-acceptor pair transition:

$$k_{D A}^0 = (k_{D X}^0 - k_{FE}) + (k_{A X}^0 - k_{FE}) \quad (2.20)$$

where $k_{D A}^0$, $k_{D X}^0$, k_{FE} and $k_{A X}^0$ denote the slopes of $\log(I_{D A}^0)$ vs $\log(L)$, $\log(k_{D X}^0)$ vs $\log(L)$, $\log(k_{FE})$ vs $\log(L)$ and $\log(k_{A X}^0)$ vs $\log(L)$ graphs, respectively.

As a result of all calculations made above, we can say that this model can satisfactorily reproduce the power dependence of all photoluminescence lines. This dependence of photoluminescence lines on laser excitation power can be described by the simple power law of the form $I \sim L^k$, when L is varied over a range of less than two orders in magnitude. According to this result, the coefficient k is generally $1 < k < 2$ for the free- and bound-exciton emission and $k < 1$ for the free-to-bound and donor-acceptor pair transition. There is no restriction for this model to apply for particular semiconductor.

2.4.4 Dependence of the Peak Energy of the Donor-Acceptor Pair Photoluminescence Band on Excitation Intensity

In photoluminescence experiments, it is generally observed and accepted that emission band peak shifts to higher energies when the laser excitation intensity is increased. To formulate this behavior, several attempts were made. M. I. Nathan and T. N. Morgan [38] obtained the following relation, explaining the dependence of the emission band

peak energy shift on excitation laser intensity:

$$L(\nu) = L_0 \exp(h\nu/E_0) \quad (2.21)$$

where $h\nu$ is the peak energy maximum of the photoluminescence band, L_0 is a constant and E_0 is a coefficient which depends on the compensation of the sample. This coefficient becomes very small in non-compensated samples, where there is no shift in emission band peak.

D. G. Thomas *et al.* [39] have also tried to examine the dependence of the shift in photoluminescence band peak on the laser excitation intensity for GaP sample. They have plotted laser excitation intensity versus photoluminescence band peak energy graph in logarithmic scale and tried to fit a straight line to the widely scattered experimental data points. However, it has been found that there is an obvious deviation of the experimental data from a straight line [40]. P. J. Dean and J. L. Merz also observed this deviation from the straight line in their work for ZnSe sample [41].

E. Zacks and A. Halperin [42] derived an analytical expression for the dependence of the peak energy of the photoluminescence band laser excitation intensity. They considered a sample with dielectric constant ϵ and with donor and acceptor concentrations N_D and N_A , respectively. They also considered one of these concentrations in minority and the other is in majority, for example, $N_D \ll N_A$. They made the assumption that the temperature of the crystal is so low that thermal ionization of the impurities is negligible. Any pair recombination will leave an ionized donor-acceptor pair of separation of r , typically a nearest neighbor pair. Excitation process, for

example, by light producing band-to-band transition, produces free charge carriers. These carriers eventually get captured by ionized impurities and turns them back to the neutral state.

The light intensity, which is emitted by the recombination of donor-acceptor pairs having separations r and $r+dr$, should be proportional to the concentration of neutral minority impurities, $N_D P(r)$, to the number of majority impurities in the volume element $4\pi r^2 dr$, and to the rate of the pair recombination $W(r)$. $P(r)$ is the fraction of neutral donors and $W(r) = 1/\tau(r)$, where $\tau(r)$ is the lifetime of the pairs. In appropriate intensity units, this light intensity can be written as

$$I(r) = 4\pi N_a N_d r^2 P(r) / \tau(r) . \quad (2.22)$$

On continuous excitation, a steady state will be reached when the rate of the generation of neutral pairs will just be equal to the rate of their recombination. A given intensity of the exciting light will produce a constant flux of free carriers, M , at steady-state. The rate of excitation can be written with the capture cross section for an electron or a hole of the ionized donor-acceptor pair, $\sigma(r)$, as follows

$$W_{\text{exc}} = 1/\Gamma(r) = M \sigma(r) \quad (2.23)$$

where $\Gamma(r)$ is the lifetime of unexcited pair under the given conditions of excitation.

At steady state,

$$P(r)/\tau(r) = [1-P(r)]/T(r) \quad (2.24)$$

or

$$P(r) = \tau(r)/[\tau(r) + T(r)]. \quad (2.25)$$

After substituting $P(r)$ into the Eqn. (2.22) it is found that

$$I(r) = 4\pi N_A N_D r^2 / [\tau(r) + T(r)]. \quad (2.26)$$

Taking the zero energy as $E_g - E_D - E_A$, following relations are obtained

$$E(r) = -e^2/\epsilon(r) \quad (2.27)$$

$$dE = (e^2/\epsilon(r)r^2)dr \quad (2.28)$$

so that

$$I(E) = 4\pi N_A N_D (e^2/\epsilon)^3 / E^4 [\tau(E) + T(E)] \quad (2.29)$$

To obtain the analytical form of the recombination rate, it is assumed that one of the impurities produces a shallow hydrogenic energy level and the other produces a much deeper one. Under this condition, the recombination rate is given by a good approximation as the following relation

$$W(r) = W_0 e^{-2r/R_B} \quad (2.30)$$

where W_0 is a constant and R_B is the shallow impurity Bohr radius. Using Eqn. (2.27) and setting $E_B = e^2/\epsilon R_B$, it is found that

$$W(E) = 1/\tau(E) = W_0 e^{-2E_B/E} \quad (2.31)$$

The dependence of the capture cross section on separation has been estimated previously [43-45] to be

$$\sigma(r) = A r^2 \quad (2.32)$$

Now, substituting Eqn. (2.23), (2.27), (2.28), (2.31) and (2.32) into (2.29) and taking the derivative of (2.24) or (2.25) with respect to E and equating to zero to obtain energy maximum intensity E_m , the following relation was obtained

$$T(E_m)/\tau(E_m) = \frac{1}{3} (E_B/E_m)^{-2} \quad (2.33)$$

Finally, by inserting the expressions for $T(E_m)$ and $\tau(E_m)$ from Eqn. (2.23), (2.31) and (2.32) and remembering that the flux of the excited carriers M is proportional to the excitation intensity L , we obtain the expression for L as

$$L = D [E_m^3 / (E_B - 2E_m)] e^{-2E_B / E_m} \quad (2.34)$$

where D is a proportionality factor.

It is obvious from the Eqn. (2.34) that the band maximum shifts to higher energies with increasing laser excitation intensity as expected. To compare with the experimental results, it is better to use the measured photon energies instead of $E(r)$, so that

$$E_m = h\nu_m - h\nu_\infty \quad (2.35)$$

$$E_B = h\nu_B - h\nu_\infty. \quad (2.36)$$

Rewriting Eqn. (2.34), following expression is found

$$L = D \frac{(h\nu_m - h\nu_\infty)^3}{h\nu_B + h\nu_\infty - 2h\nu_m} \exp\left(-\frac{2(h\nu_B - h\nu_\infty)}{h\nu_m - h\nu_\infty}\right). \quad (2.37)$$

There are three free parameters in this equation, D , $h\nu_B$ and $h\nu_\infty$. Here D is an only a proportionality factor and for this reason its calculated values are not important in this

calculations. The other two parameters $h\nu_B$ and $h\nu_\infty$ have special importance while interpreting the experimental results.



CHAPTER 3

EXPERIMENTAL TECHNIQUES USED IN PHOTOLUMINESCENCE EXPERIMENTS

3.1 Experimental Setup Used in Photoluminescence Experiments

In photoluminescence experiments, the setup shown in the figure (3.1) was used

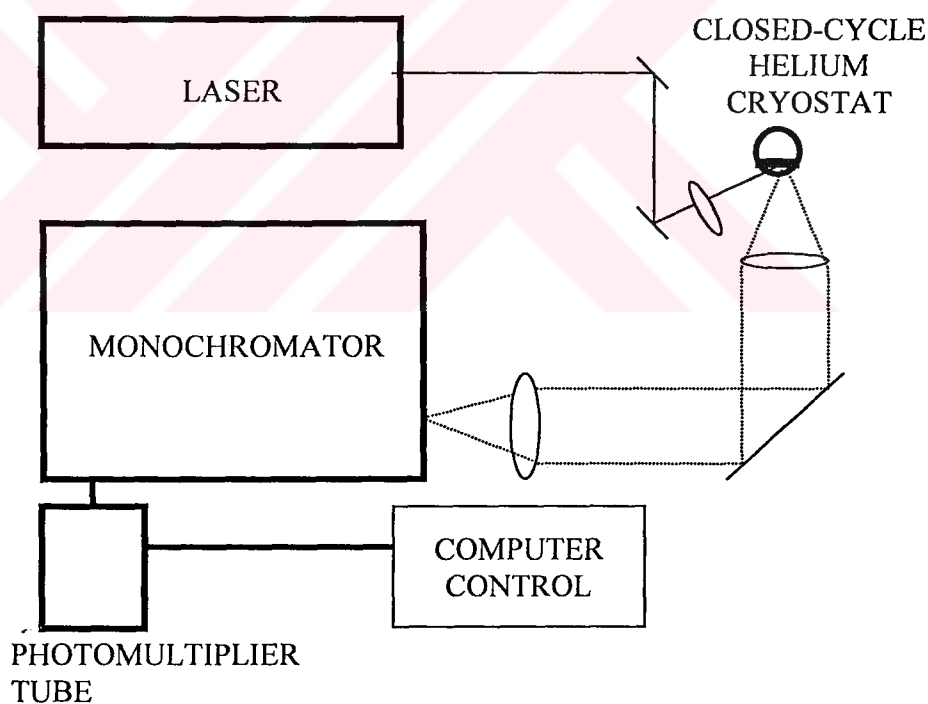


Fig. 3.1 Schematic diagram of photoluminescence setup used in experiments

"Spectra-Physics" He-Ne and an Ar ion lasers operating at wavelengths of 632.8, 514.5 and 488.0 nm were used appropriately as the excitation light source depending on the band gap energy and the excitonic structure of each sample. A "CTI-Cryogenics M-22" closed-cycle helium cryostat was used to cool the crystals from room temperature down to 10 K. The temperature was controlled within an accuracy of ± 0.5 K. The PL spectra were analysed using a "Jobin-Yvon" U-1000 double-grating spectrometer and a cooled GaAs photomultiplier equipped with the necessary photon counting electronics. A cylindrical lens was used in front of the sample to minimize the damage on the sample and a collective lens was used to collect the PL signal from the sample. To adjust the value of excitation laser intensity, a set of neutral-density filters was used. The computer control system was used to control the experimental setup and record the PL data.

3.2 Experimental Techniques Used in Photoluminescence Experiments

In the experiments, all of the samples were prepared by cleaving an ingot parallel to the crystal layer, which was perpendicular to the *c*-axis. The surfaces of the samples were freshly cleaved just prior to loading them onto the cold finger of the closed-cycle refrigerator. In all of the experiments, the carrier types of the studied samples were determined by the hot-probe method. The PL was observed from the laser-illuminated face of the samples. All photoluminescence spectra were recorded when the system temperature was stabilized around desired value, which usually requires approximately 15 – 20 minutes. All spectra have been corrected for the spectral response of the optical apparatus and photodetector. All spectra have been analysed by a using fitting procedure

to deconvolve the complex bands. To do this, we used the Peakfit program. In Fig. 3.2, the usage of this program to deconvolve the experimental photoluminescence spectra into separate peaks is shown.

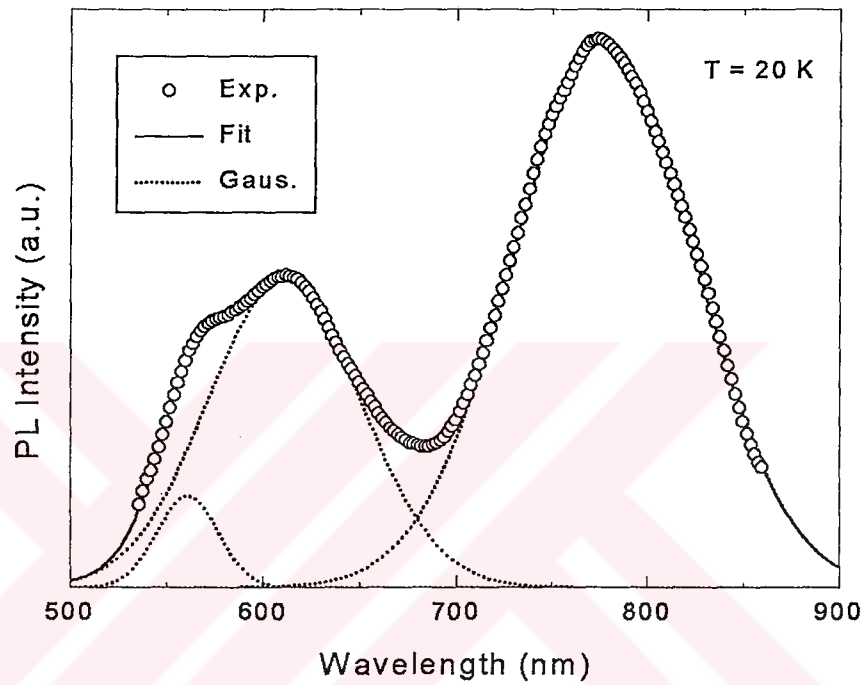


Fig. 3.2 Deconvolution of the photoluminescence spectra into two Gaussian lineshapes

CHAPTER 4

RESULTS AND DISCUSSION

4.1 Introduction

In this part, we will deal with the details of photoluminescence experiments for each of the three crystals (GaS, GaS_{0.5}Se_{0.5}, GaSe). We will also give some results and conclusions for each of the samples independent from each other.

4.2 Results and Discussion of the PL Experiment for GaS crystal

4.2.1 Experimental Details

Gallium sulfide polycrystals were synthesized from high purity (at least 99.999%) gallium and sulfur taken in stoichiometric proportions. Single crystals of GaS were grown by the modified Bridgman method. X-ray diffraction analysis of the data showed that GaS crystallizes in the hexagonal unit cell with lattice parameters of $a = 0.359$ and $c = 1.549$ nm [46]. Crystals suitable for measurements were obtained by easy cleavage along the (001) plane perpendicular to the optical c -axis. As-grown GaS is an n -type semiconductor having an indirect energy band gap of 2.591 eV at 77 K and 2.597 eV at 4.2 K [4].

Photoluminescence experiments on GaS were made from the cleaved surfaces of the crystals in a back scattering configuration in the wavelength range of 525-860 nm. The 457.9 nm (2.71 eV) line of an argon ion laser was used as the exciting light source. Sets of neutral density filters were used to adjust the exciting laser intensity from 0.0007 to 8.0931 W cm⁻², a factor of more than 10⁴.

4.2.2 Results and Discussion

PL spectra of GaS in the 525-860 nm wavelength and 9-280 K temperature range at a constant excitation intensity are shown in Fig. 4.1. We observe three broad PL bands centered at 558 nm (2.22 eV, A-band), 614 nm (2.02 eV, B-band) and 780 nm (1.59 eV, C-band) at 9 K. We note that both the PL intensities and the PL peak energies change as a function of increasing sample temperature. As the temperature of the sample is increased, PL intensity of all three bands decreases. However, while at higher temperatures, the two short wavelength peaks disappear altogether, the intensity of the third band in the near infrared part of the spectrum increases for a narrow range of temperatures from 90-150 K, followed by a decrease of the PL intensity. The observed peak energies of the two short wavelength bands at 9 K shift towards the red continuously as the temperature is increased, until they are totally quenched, whereas the third band shifts towards the blue until 130 K followed by a red shift thereafter. Despite this peculiarity of the near infrared band, these features are indicative of donor-acceptor pair transitions observed in many ternary semiconductors. All data has been analyzed by fitting three Gaussian lineshapes, for $T = 20$ K, from which peak intensity, peak position and the full width at half maximum (FWHM) of all three bands were obtained.

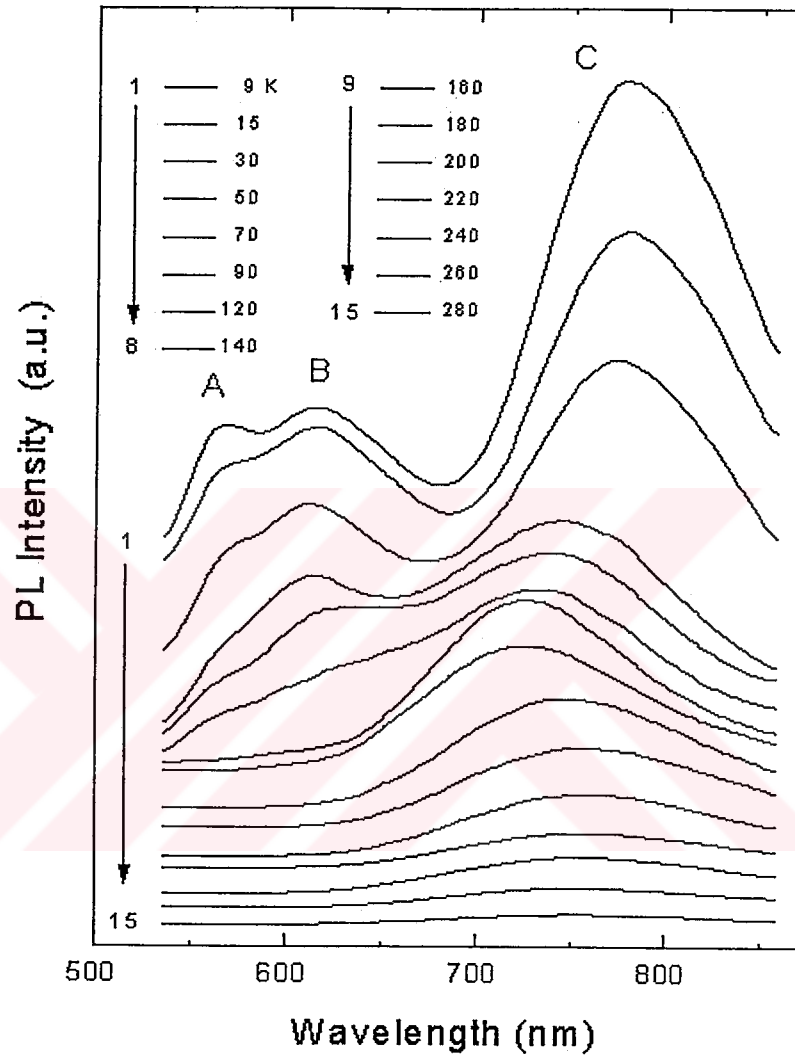


Fig. 4.1. Temperature dependence of PL spectra from GaS single crystal in the 525–860 nm range

The variations of the PL peak intensity of all three bands with respect to temperature are plotted in Fig. 4.2. In the low temperature range, PL intensity of the A- and the B-bands decrease slowly. Above 60 K for the A-band and 50 K for the B-band, however, the peak intensity decreases at a much larger rate due to a thermal quenching process. A similar behavior is observed for the C-band which decreases slowly in the 9-90 K range and except for a small range of temperatures between 90-150 K, where it increases, it decreases much more sharply above 150 K. The small increase in the PL emission intensity between 90-150 K is due to redistribution of carriers as both A- and B-bands totally quench. The activation energies for all three bands have been obtained by fitting to the following equation:

$$I = I_0 \exp (\Delta E / k_B T) \quad (4.1)$$

where I is the PL intensity, I_0 is proportionality constant and k_B is the Boltzmann's constant. The semilog plot of the peak intensity as a function of the reciprocal temperature gives a straight line for all three bands at low temperatures, the slopes of which give the activation energies as 0.017, 0.013 and 0.151 eV for A-band, B-band and C-bands, respectively. Since, as-grown GaS is an n -type semiconductor as confirmed by the measurement of the carrier type by the hot probe method, we consider that the activation energies of 0.017 eV and 0.013 eV are associated with donor levels. As will be shown shortly, the temperature dependencies of the PL peak energy and FWHM of the C-band are different from the others which lead us to explain the behavior of this band within the configuration coordinate (CC) model [47]. Therefore, the activation

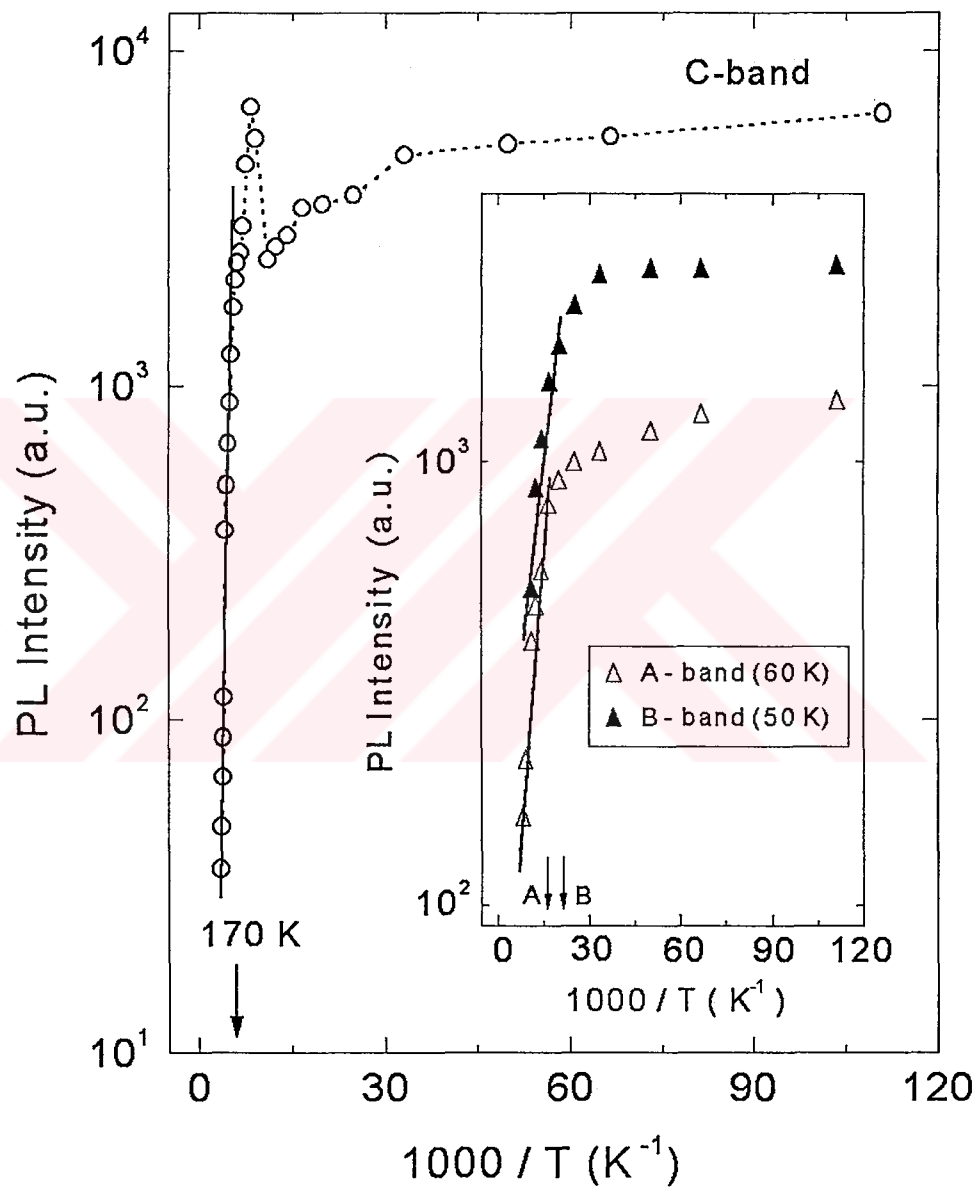


Fig. 4.2 Temperature dependence of the peak intensity of A, B, and C bands. The arrows show the starting points of the intensive quenching

energy derived from Fig. 4.2 for the C-band is associated with the difference between the minimum of the excited state and the intersection point of the excited and ground state CC curves.

Temperature dependence of the peak energy for all three bands is plotted in Fig. 4.3. Both A- and B-bands show a small red shift as the temperature increases. Full temperature dependence of the band gap of GaS is not available in the literature but it is known that the temperature coefficient of the band gap energy of GaS is negative [4]. Therefore, the peak energy due to donor-acceptor pair recombination should also decrease as the temperature increases. The observed shift of the peak energy position towards lower energies satisfies the temperature dependence expected for donor-acceptor recombination for these bands. Similar behavior is observed in many binary and ternary semiconductors [20,48]. As seen in Fig. 4.3, temperature dependence of C-band, however, shows totally different behavior. Instead of the red shift observed as in the cases of A- and B-bands, peak energy of the C-band, starting at 1.59 eV (at 9 K), blue shifts rapidly between 25-50 K and continues to blue shift beyond 50 K until 130 K albeit at a smaller rate until it reaches a peak value of 1.71 eV. The total blue shift observed is approximately 120 meV, in this temperature range. Beyond 130 K, peak energy of the C-band, red shifts back, reaching to 1.62 eV at 190 K, larger than what is observed at the lowest temperature. In fact, the peak energy value does show yet a second blue shift beyond 200 K up until 280 K, where the intensity of the C-band becomes very low. To our knowledge, this is the first time such a complex behavior is observed in the PL spectra of GaS or its related layered semiconductors. Blue shifting of the peak energy of an emission from semiconductors has previously been studied within the framework of the configuration coordinate model where a ground state is associated

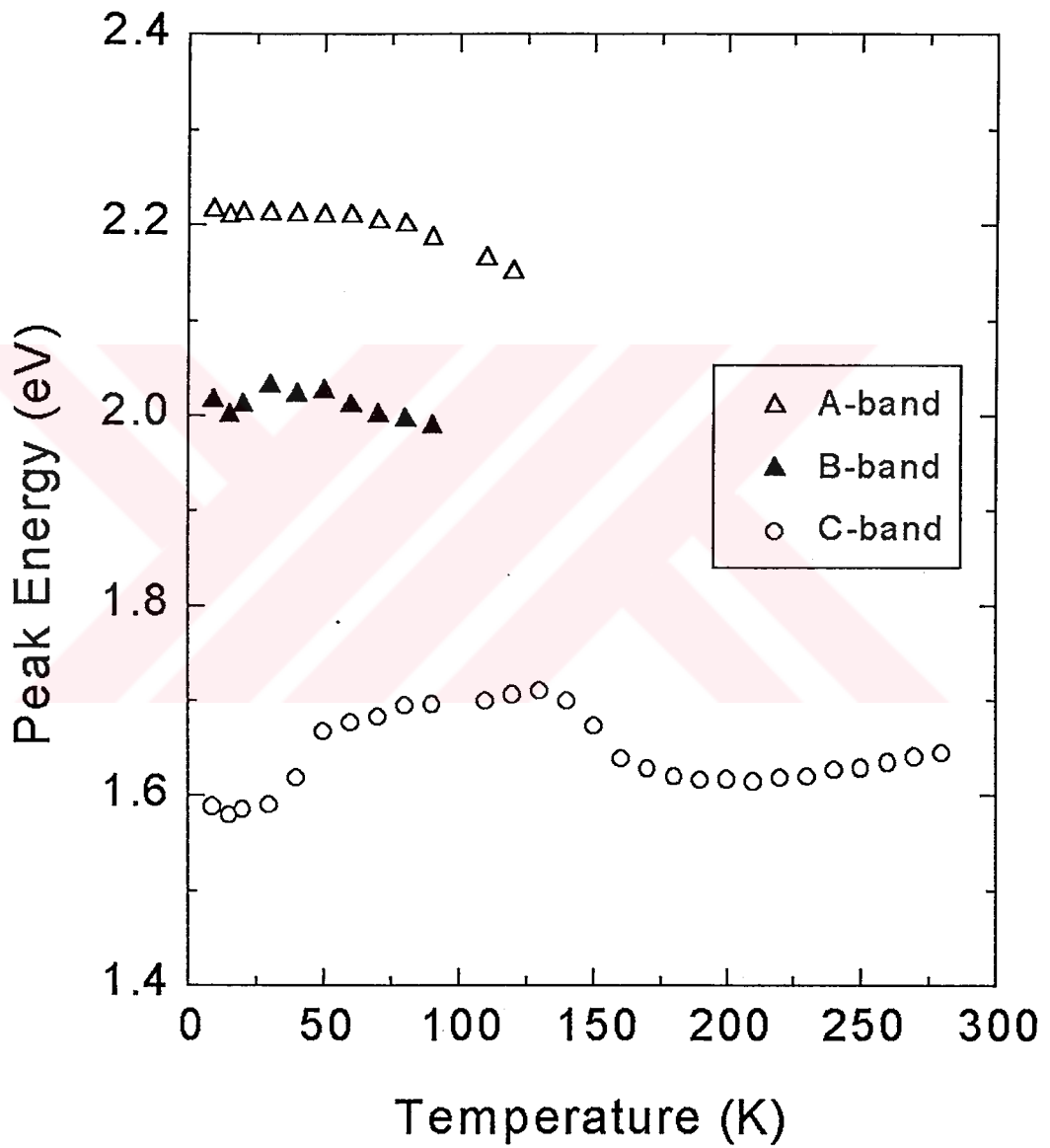


Fig. 4.3 Temperature dependence of the peak energy of bands A, B, and C

with an acceptor level and an excited state is derived from a donor level situated in the band gap of the crystal. Before we discuss our data within this model, we present the temperature dependence of the FWHM of the C-band, W , which appears to follow the CC model equation [47]

$$W = W_0 [\coth (h\nu_e / 2k_B T)]^{1/2}, \quad (4.2)$$

where W_0 is a constant, whose value is equal to W as the temperature approaches 0 K and $h\nu_e$ is the energy of the vibrational mode of the excited state. The result of the analysis is shown in Fig. 4.4. The FWHM of the C-band shows two distinct behaviors. At lowest temperatures, it has a value of 0.28 eV. As the temperature increases, FWHM shows rapid increase until 50 K where it reaches the maximum value of 0.36 eV followed by a decrease in the FWHM in the 50-80 K range. The value of FWHM at 80 K is 0.30 eV, which is still larger than the starting value of 0.28 eV. Finally, it increases once more, but now at a slower rate than previous rate, reaching to 0.42 eV at 280 K. As is clearly seen from the data, the slopes of low- and high-temperature behavior of the FWHM are different. Using a least squares routine, we fit Eqn. (4.2) to low- and high-temperature parts of the data, separately. The fitted values of $W_0 = 0.279$ eV, $h\nu_e = 5.45$ meV for the low-temperature and $W_0 = 0.294$ eV, $h\nu_e = 25.36$ meV for high-temperature parts of Fig. 4.4 are obtained. Clearly, much higher values of $h\nu_e$ are associated with the high temperature behavior of the width of the C-band. Finally, we have also analysed the widths of both A- and B-bands and find that they do not show any significant temperature dependence as does the C-band.

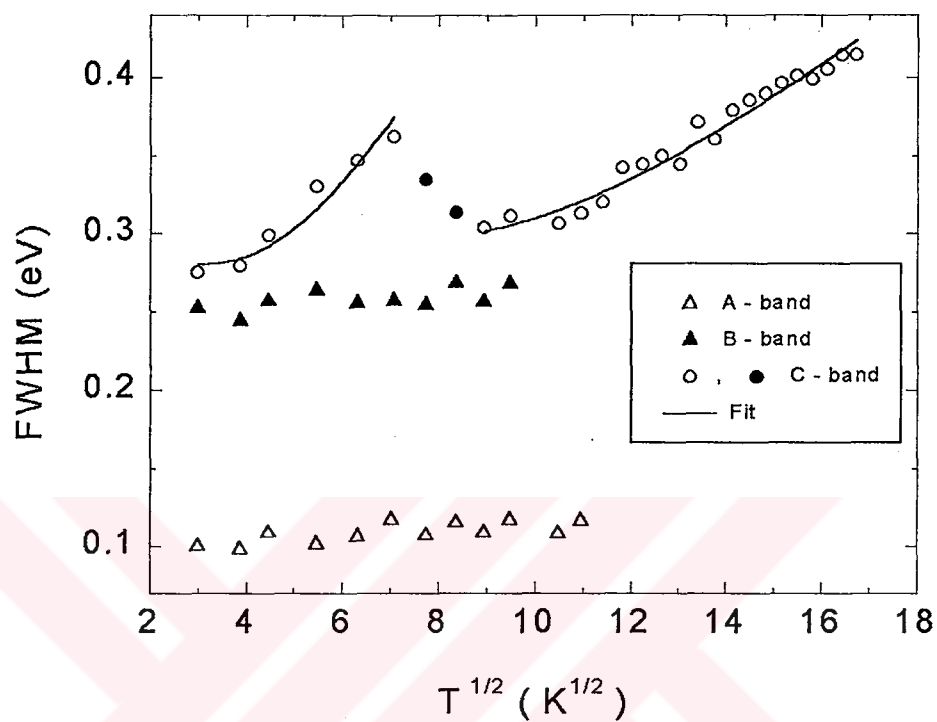


Fig. 4.4. Linewidths of the A, B, and C bands as a function of the square root of temperature

In elucidating the nature of deep level luminescence from semiconductors, excitation laser intensity dependence of the PL spectra is an important consideration. In Fig. 4.5, we present the excitation laser intensity dependence of the PL spectra of GaS. All three bands are visible even at the lowest excitation intensity and increase in intensity as the excitation intensity increases. Detailed analysis of the peak positions of all three bands, as a function of increasing excitation laser intensity did not yield any variation of the peak energy values of any of the bands. We, therefore, concentrated on the analysis of PL intensity as a function of the excitation laser intensity. Excluding the

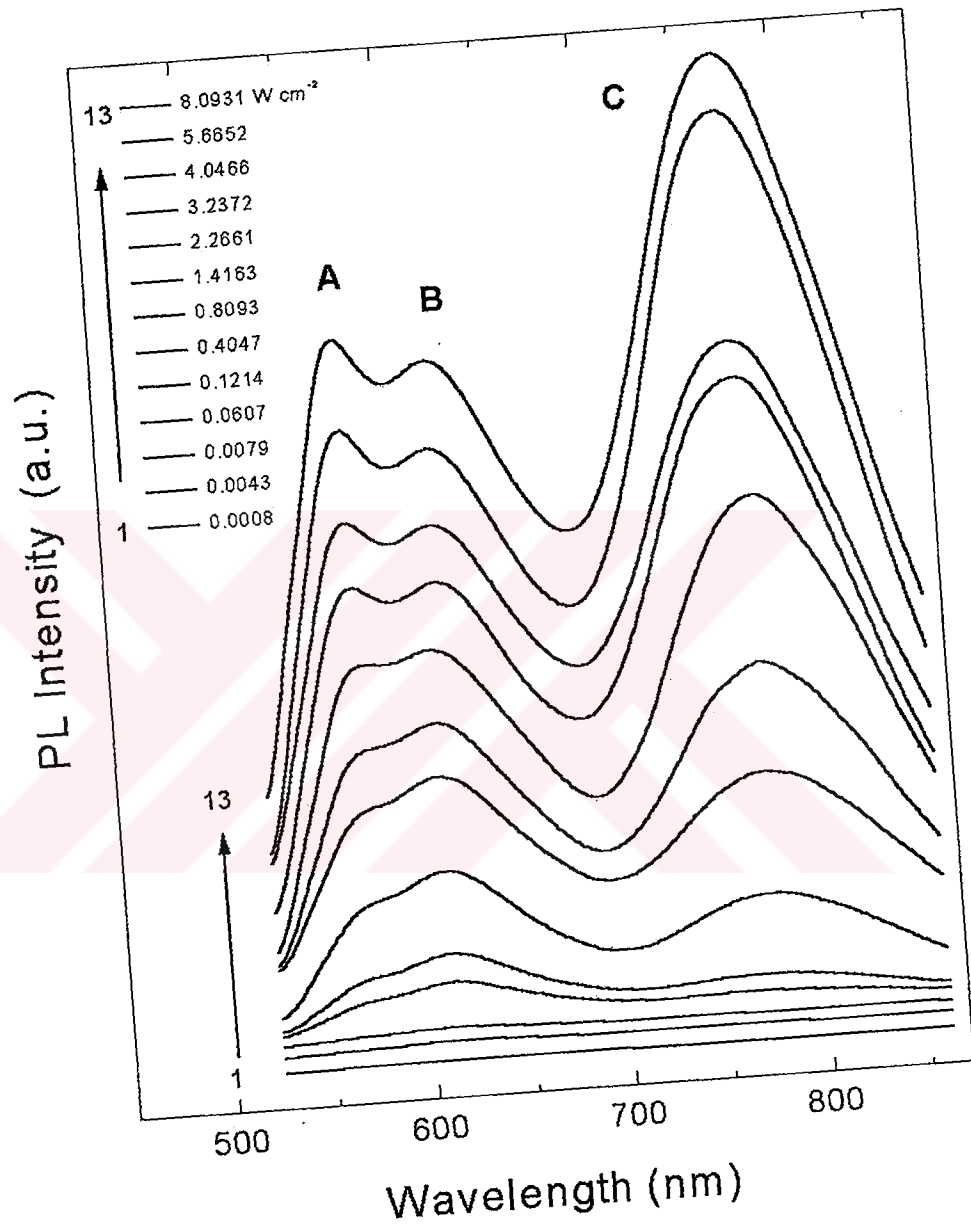


Fig. 4.5 Excitation intensity dependence of the photoluminescence spectra of GaS at $T = 9\text{ K}$

very high intensity region where there is clear saturation of the PL intensity, analysis has been carried out by fitting the experimental data to a simple power law of the form Eqn. (2.7) (Fig. 2.6). It was found that the maximum PL intensity of the emission band increases sublinearly with respect to the excitation laser intensity for all three bands. The values of k were found 0.86, 0.80, and 0.88 for A-, B- and C-bands, respectively. Saturation starts at $L > 0.41 \text{ W cm}^{-2}$ for B-band, at $L > 3.24 \text{ W cm}^{-2}$ for A- and C-bands. It is well known that for excitation laser photon with an energy exceeding the bandgap energy, E_g , the coefficient k is generally $1 < k < 2$ for the free- and bound-exciton emission, and $k \leq 1$ for free-to-bound and donor-acceptor pair recombinations [37]. Thus, the obtained values of $k < 1$ for all three bands further confirms our assertion that all three bands in the PL spectra of GaS are due to donor-acceptor pair recombinations.

From the above data, it is clear that there are two types of behavior in the PL spectrum of GaS: one, is the behavior of bands A and B; the other is the behavior of the C-band. The two short wavelength bands A and B show quenching at relatively low temperatures of 60 and 50 K, respectively, with no significant change in the width of their bands. Peak energy of both bands show a small decrease with increasing temperature but do not change with increasing excitation laser intensity. While the former result is typical of donor-acceptor pair recombination process, the latter result rules out the model of "distant" donor-acceptor pair recombination (DAP) process where a shift toward higher energies are expected as the excitation laser intensity is increased [31]. It is known that in general, the emission energy from a DA pair separated by a distance of r is obtained from [49]

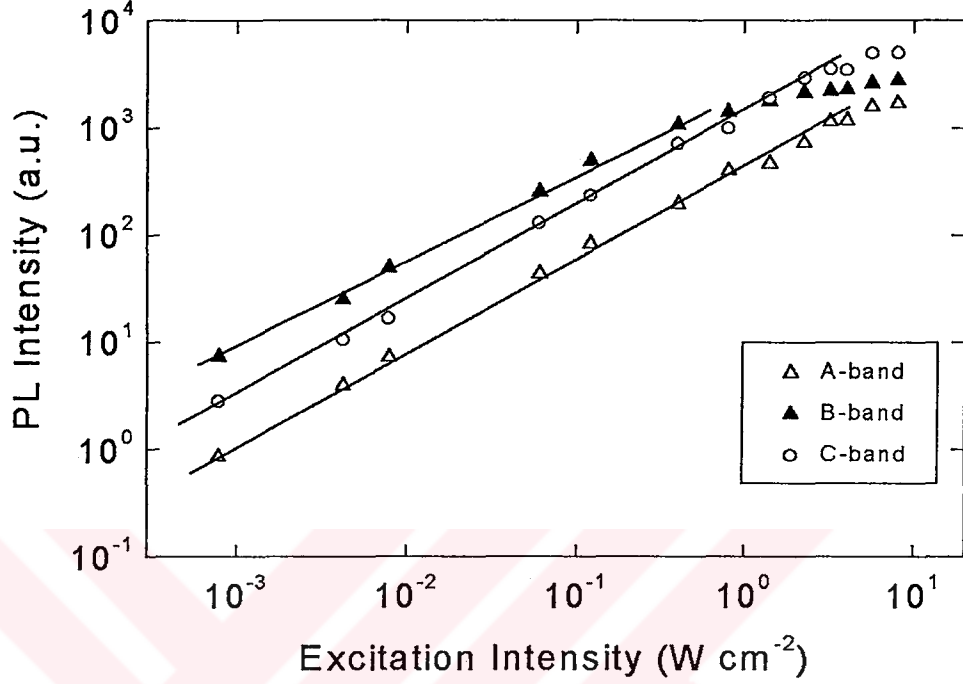


Fig. 4.6. Excitation intensity dependence of the peak photoluminescence intensity of bands A, B, and C

$$E(r) = E_g - (E_A^0 + E_D^0) + \frac{Z_D Z_A e^2}{\epsilon r} - \Gamma(r), \quad (4.3)$$

where, E_g is the band gap energy, E_A^0 and E_D^0 are the acceptor and donor ionisation energies, ϵ is the dielectric constant, Z_D and Z_A are the charges of the donor and acceptor states, respectively. $\Gamma(r)$ is a quantum mechanical correction representing the interactions at very short distances. Since, this term gives only second order correction and only at very short distances, we will neglect it in our discussion. However, the value of $\Gamma(r)$ at very short distances may be as high as 25 meV in some cases [50] so that

theoretically calculated and experimentally determined values of Coulombic energies may differ significantly.

From Eqn. (4.3), two features of the observed data become clear. First, increase in pair separation r , and the pairs that are apart play role in the recombination process. Because of this, the peak energies should shift to lower energies in addition to the shrinking of the band gap [51]. Second, it is also clear that as the excitation laser intensity is increased, the contribution of closer pairs will increase leading to the expected blue shift of the peak energy of the emission. Since this is in contrast with the observed data, we conclude that, only close pairs such as the nearest or next-nearest neighbors are involved in the transitions. This assumption is further supported by the fact that observed decrease of the peak energy of both A- and B-bands is indeed relatively small suggesting that pairs far apart contribute little to the observed emission.

Unfortunately, there is little data on the nature of defect states in GaS that will help identify possible defect complexes involved in the observed recombination processes. Aono [10] studied GaS crystals grown by the iodine transport method, where iodine highly substitutes a sulfur site and acts as a donor and where, from charge neutrality arguments, production of gallium vacancies with two charge states, V_{Ga}^{+2} and V_{Ga}^{+1} was assumed. Furthermore, the existence of V_{Ga}^{+2} is understood to be an excited state of V_{Ga}^{+1} when it releases an electron. Thus, the energy level of V_{Ga}^{+2} should be higher than that of V_{Ga}^{+1} above the valence band edge. In general, one should consider all combinations of vacancies and interstitials for both gallium and sulfur in GaS as possible sites of recombination. Due to the binary nature of the crystal, the possible number of such pairs is limited. However, different charge states may increase this

number. It is possible that a gallium vacancy with different charge states and sulfur interstitial are involved in these transitions but more data is required before a firm conclusion can be made.

Recently Krustok [49] suggested that it may be possible to guess the positions of the defect states involved in DAP recombinations by calculating the energy separation of the observed bands. Assuming that only the nearest neighbor or next-nearest neighbor lattice sites are involved, we compare a pair such as Ga-S with another such as (i)-S, where (i) represents an interstitial position. Here, Ga and S represent the lattice sites, which behave as acceptor and the donor sites. Again, assuming that the acceptor and donor energies as well as the quantum mechanical correction term, $I(r)$, for both pairs are approximately the same, one finds the energy separation of two bands as:

$$\Delta E = \frac{Z_A Z_D e^2}{\epsilon} \left(\frac{1}{r_1} - \frac{1}{r_2} \right), \quad (4.4)$$

where Z_A and Z_D are the charge states of the acceptor and donor sites, r_1 and r_2 represent the pair separation of each pair, e is the electronic charge and ϵ is a combination of optical and static dielectric constants [49]. However, exact numerical value for ϵ is hard to predict not only because the exact combination of optical and static dielectric constants are not known but GaS has two dielectric constants, one parallel to the c -axis, the other perpendicular to it. Furthermore, there may be lattice distortion associated with defect sites, which would introduce further errors into the calculations. Despite the uncertainties associated with using Eqn. (4.4), we find that only the nearest neighbor

pairs and interstitial sites give reasonably close values to the observed energy separation (ΔE) of 200 meV, 430 meV and 630 meV between A- and B-, B- and C-, and A- and C-bands, respectively. Comparison of nearest neighbor pairs with distant neighbors result in energy separation values on the order of few eV, clearly beyond what is observed experimentally. In these calculations, we used $Z_A = 1$ and $Z_D = 1$ and the larger of the dielectric constants which is the one perpendicular to the c -axis, $\epsilon = 9.5$ [52], but using any value smaller than 9.5 would not change our overall conclusion since ΔE is inversely proportional to ϵ .

Sublinear dependence of the PL intensity on the excitation laser intensity is also consistent with donor-acceptor pair recombination process since the simultaneous solution of the rate equations involving all possible radiative transitions give sublinear dependence for free-to-bound and donor-acceptor pair recombinations [20]. We summarize the results for A- and B-bands in Fig. 4.7 Using the activation energies obtained from the temperature dependence of the PL intensity for n -type GaS, we place donor levels d_1 and d_2 at 0.017 eV and 0.013 eV below the conduction band. From the peak energy values of the observed transitions, the related acceptor energy levels a_1 and a_2 are then placed at 0.363 and 0.568 eV above the valence band. Thus, our DA pairs for A- and B-bands are composed of deep acceptor and shallow donor states.

The most striking feature of the C-band is the temperature dependence of its peak energy. As seen in Fig. 4.3, in contrast with A- and B-bands, the peak energy of the C-band increases by almost 120 meV until 130 K is reached followed by a red shift. Such behavior is classically understood in terms of the configuration coordinate model of defects [47]. In Fig. 4.7, we present our configuration coordinate model for the C-band.

In this model, the ground state of the system is derived from a deep acceptor level while the excited level is associated with a donor level. Since $A^{III}B^{VI}$ -type layered crystals are more polar than covalent [53], the displacement of the excited state minimum is expected to be reasonably large. The quantum mechanical treatment of the configuration coordinate model leads to quantised states associated with each level. The initial blue shift of the peak energy with increasing temperature is understood by the transitions from higher states in the excited level as the occupation of these states increase with temperature. From the bandwidth data, we deduce that FWHM and hence

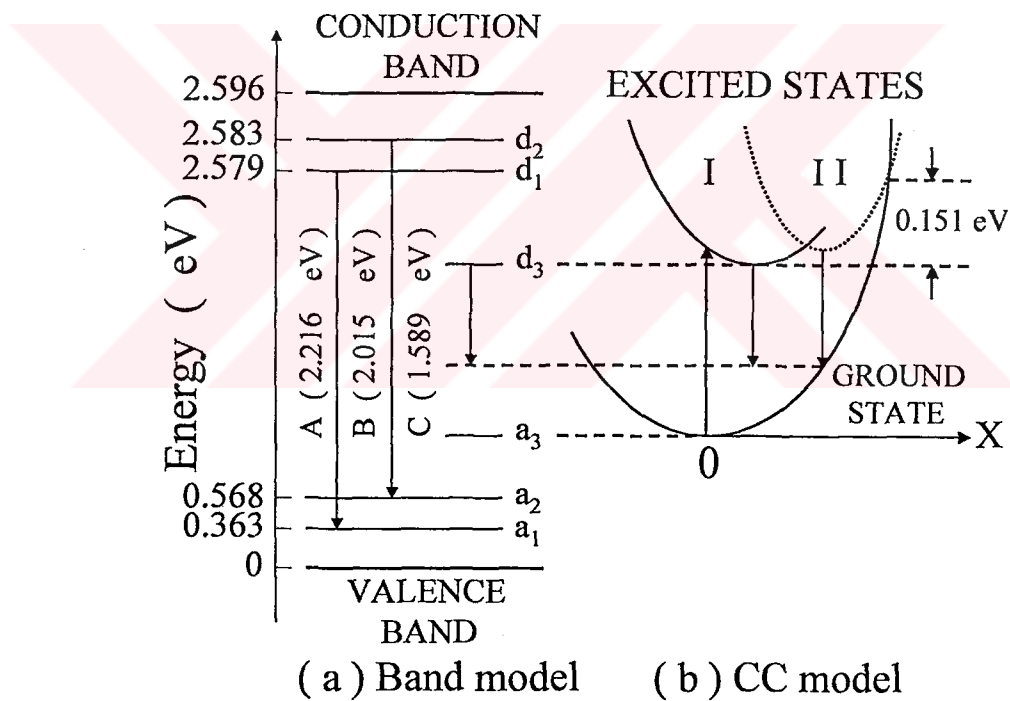


Fig. 4.7 Proposed model for the donor-acceptor pair recombination processes in GaS at $T = 9 \text{ K}$

the energy of the excited state, $h\nu_e$, involved in the emission, change in the temperature range 50-80 K. While, $h\nu_e$ is about 5 meV below 50 K, it becomes 25 meV above 80 K.

This suggests the presence of a higher excited state. This is shown as a second excited state next to the first one in Fig. 4.7. Blue shifting of the peak energy continues to increase up to 130 K in this second excited state. In this model, the red shift beyond 130 K is understood by the filling of the lowest ground state. The slow blue shift following the red shift is also understood yet by further filling of the second excited state. Finally, the thermal quenching occurs when the carrier energy is large enough, so that it can relax to the ground state with a nonradiative transition at the intersection of the ground and excited state energies. It is possible to construct more complicated CC models, however, we find that this is the simplest model that seems account for all the observed features of the photoluminescence from GaS.

4.2.3 Conclusions

We measured low temperature PL spectra of high quality GaS single crystals grown by the vertical Bridgman method. At 9 K, three PL bands at 2.22 eV (A-band), 2.02 eV (B-band), and 1.59 eV (C-band) have been observed. Both the excitation intensity and temperature dependencies of the bands suggest that nearest neighbor pairs are responsible for the emissions. Deep acceptor and shallow donor levels in the band gap of GaS account for the observed emission for A- and B-bands. The peculiar behavior of the C-band is understood within the framework of a proposed configuration coordinate model. The changes in the FWHM of the C-band as a function of temperature imply that there may be two excited states. As the samples are not intentionally doped, donor and acceptor states are thought to originate from point defects.

4.3 Results and Discussion of the PL Experiment for GaS_{0.5}Se_{0.5} crystal

4.3.1 Experimental Details

Single crystals of GaS_{0.5}Se_{0.5} were grown by the modified Bridgman method. The analysis of X-ray diffraction data showed that GaS_{0.5}Se_{0.5} crystallized in a hexagonal unit cell, with lattice parameters: $a = 0.3671$ and $c = 1.5719$ nm [46]. Typical sample dimensions were $4 \times 3 \times 0.7$ mm³. The studied samples were *n*-type as determined by the hot probe method. A "Spectra-Physics" argon ion laser operating at 488.0 nm was used as the excitation source. The PL was collected from the laser illuminated face, in a direction close to the normal to the *c*-axis. The PL spectra were analysed in the 565-860 nm wavelength range. A set of neutral-density filters was used to adjust the excitation laser intensity from 10^{-3} to 15.9 W cm⁻².

4.3.2 Results and Discussion

Typical deep level luminescence spectra of the GaS_{0.5}Se_{0.5} single crystals are shown in Fig. 4.8 as a function of temperature from 15 up to 170 K in the wavelength region 565-860 nm at a constant excitation density of 15.9 W cm⁻². The observed PL bands vanish above 170 K. We observe two emission bands centred at 585 nm (2.120 eV, A-band) and 640 nm (1.938 eV, B-band) in the PL spectrum at 15 K. In contrast with GaS crystal [55] there are no signs of bands in the near infrared part of the spectrum. It is seen from the spectra that the observed bands change their intensities and positions as the temperature increases. While the intensities of both bands decrease with increasing temperature, it is clear from Fig. 4.8 that A-band quenches earlier than the B-band. Both

peaks show varying degrees of red shift with increasing temperature. The full temperature dependence of the band gap of $\text{GaS}_{0.5}\text{Se}_{0.5}$ has been reported in [4-7] and the temperature coefficient of the band gap was shown to be negative. As the peak energy due to a donor-acceptor pair transition should decrease with the band gap energy, the observed red shift of the two bands is in agreement with the hypothesis of a recombination over donor-acceptor pairs.

All spectra have been analysed by a using fitting procedure to deconvolve the bands. The procedure yields the peak position, full-width at half-maximum (FWHM) and intensity of the bands. The data obtained from this analysis for the peak energy position as a function of temperature are displayed in Fig. 4.9. For comparison, the variation of the indirect band gap of $\text{GaS}_{0.5}\text{Se}_{0.5}$ as a function of temperature is also plotted. First, it should be noted that the band gap energy of $\text{GaS}_{0.5}\text{Se}_{0.5}$ does not show a large decrease upon increasing the temperature from 15 to 170 K. Furthermore, the magnitude of the observed peak energy shift for both bands is greater than that of the band gap energy with temperature while the peak energy of the A-band shows a red shift of 0.032 eV, the B-band shows a red shift of 0.130 eV. The difference in energy shift of both bands suggests that the centers responsible for the observed recombination is not necessarily the same, but similar. The observed red shift for both bands is indicative of donor-acceptor pair recombination [31] and, the observed behavior of the peak energy positions for both bands satisfies the temperature dependence expected for the donor-acceptor pair recombination. From Fig. 4.8, it is clear that the emission band intensities for both bands decrease with increasing temperature. Rapid thermal quenching is observed at temperature as low as 50 K for A-band and 90 K for B-band. The experimental data for the temperature dependence of the PL intensities at the emission

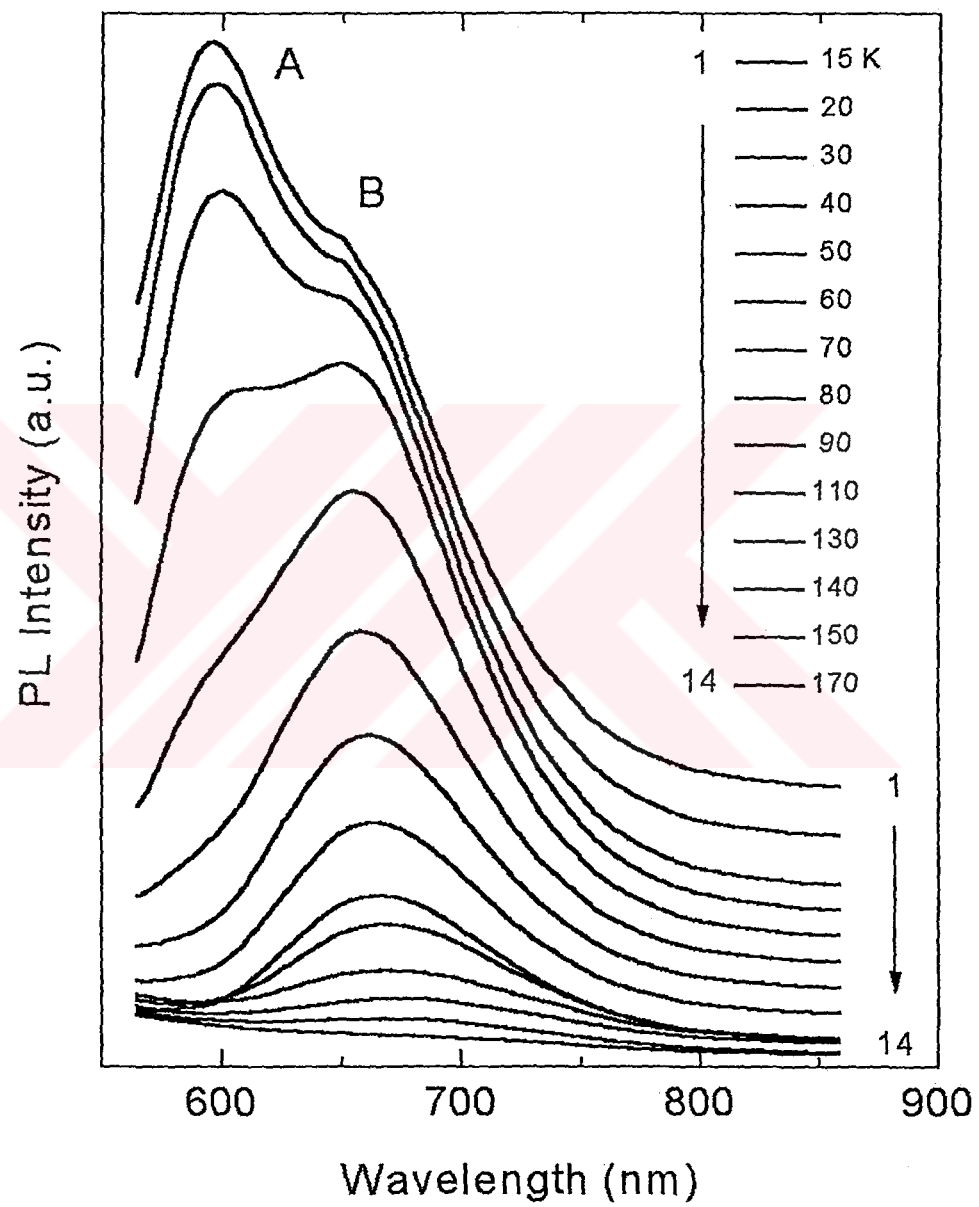


Fig. 4.8 PL spectra of GaS_{0.5}Se_{0.5} in the temperature range of 15–170 K

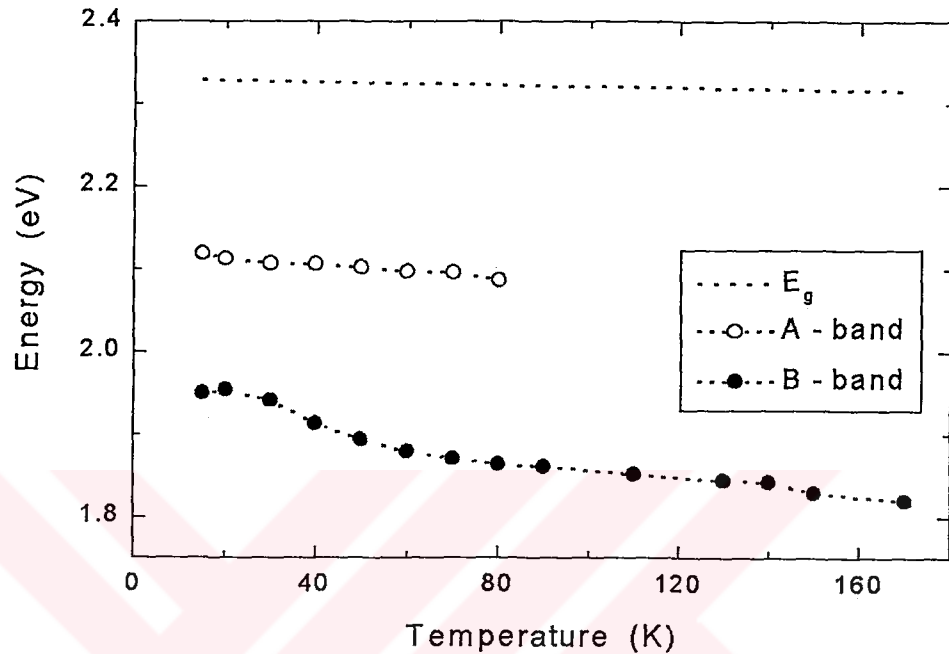


Fig. 4.9. Temperature dependencies of the E_g , A- and B-bands peak energies for $\text{GaS}_{0.5}\text{Se}_{0.5}$

band maximum can be fitted by Eqn. (4.1). Fig. 4.10 shows the temperature dependence of the emission band maximum intensity as a function of reciprocal temperature in the 15-170 K range. Fitting equation (4.1) to the high temperature parts of the plot in Fig. (4.10), we find an activation energy of about 0.029 eV for the A-band and 0.040 eV for the B-band. Since $\text{GaS}_{0.5}\text{Se}_{0.5}$ is an *n*-type semiconductor as measured by the hot probe technique, we consider that the impurity levels are donor levels located 0.029 and 0.040 eV below the bottom of the conduction band. The energy values of these donor levels are compared with two donor levels at 0.013 and 0.017 eV that we recently identified

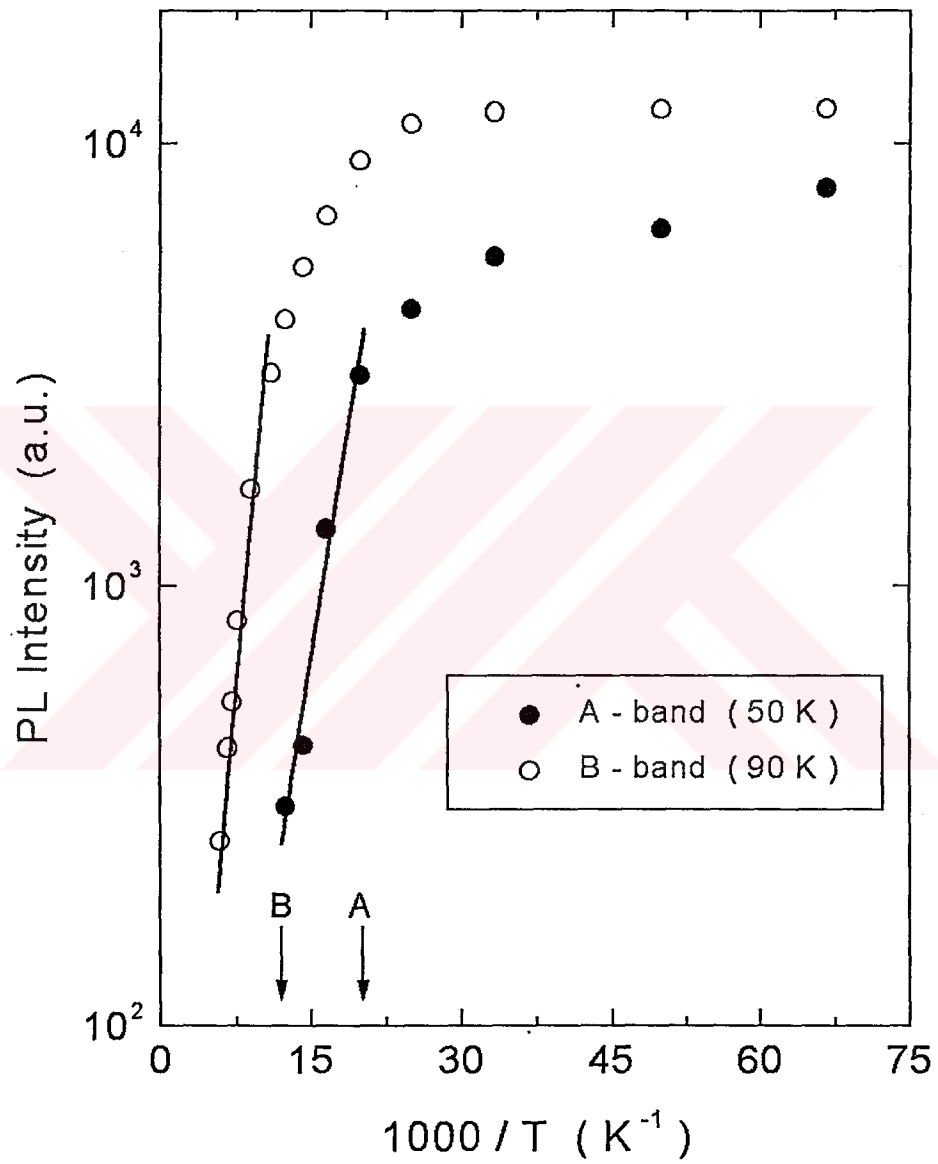


Fig. 4.10 Photoluminescence intensity of A- and B-bands at the maximum of the emission intensity as a function of reciprocal temperature, the arrows at 50 and 90 K show the starting points of intensive quenching

in the visible part of the spectrum of GaS [55]. Such shallow donor levels in $\text{GaS}_{0.5}\text{Se}_{0.5}$ may originate from deviations in stoichiometry in the form of point defects. In the past, Ga vacancies have been invoked to account for these defects as the origin of the observed PL spectra [13]. Excitation intensity dependence of the PL spectra should also provide valuable information towards identification of the recombination mechanism responsible for the observed luminescence. Deconvolution procedure also applied to spectra obtained at different excitation intensities yielded the peak energy position, FWHM and the intensity of both A- and B-bands in this case. We find that neither the FWHM nor the peak position of the bands change with increasing excitation intensity. In contrast with inhomogeneously distributed donor-acceptor pairs where increasing laser intensity excites more pairs that are closely spaced leading to blue shift of the peak energy of the observed band [31], this result suggests that the donor-acceptor pairs are located at only closely spaced sites and are distributed homogeneously. As is the case in other gallium chalcogenides, we suggest that these pairs are due to defects in the crystal. Since the calculations on the formation energy of the defect pairs suggest that formation energy of a defect pair may be lower than the sum of two individual defects formation energies, concentration of closely spaced paired defects could easily dominate in crystals such as $\text{GaS}_{0.5}\text{Se}_{0.5}$ [49]. On the other hand the intensity of the peak energy maximum increases with increasing excitation intensity which is also characteristic of donor-acceptor pair recombination. The log-log plot in Fig. 4.11 shows the excitation laser intensity dependence of the PL intensity. The experimental data can be fitted by Eqn. (2.7). We find that the PL intensity at the emission maximum increases sublinearly (i.e. $k = 0.63$ for A-band and $k = 0.51$ for B-band). It is well known that for excitation laser photon energy exceeding the band gap energy, E_g , the exponent γ is generally

$1 < k < 2$ for free and bound exciton emission, while $k \leq 1$ for free-to-bound and donor-acceptor pair recombination [37].

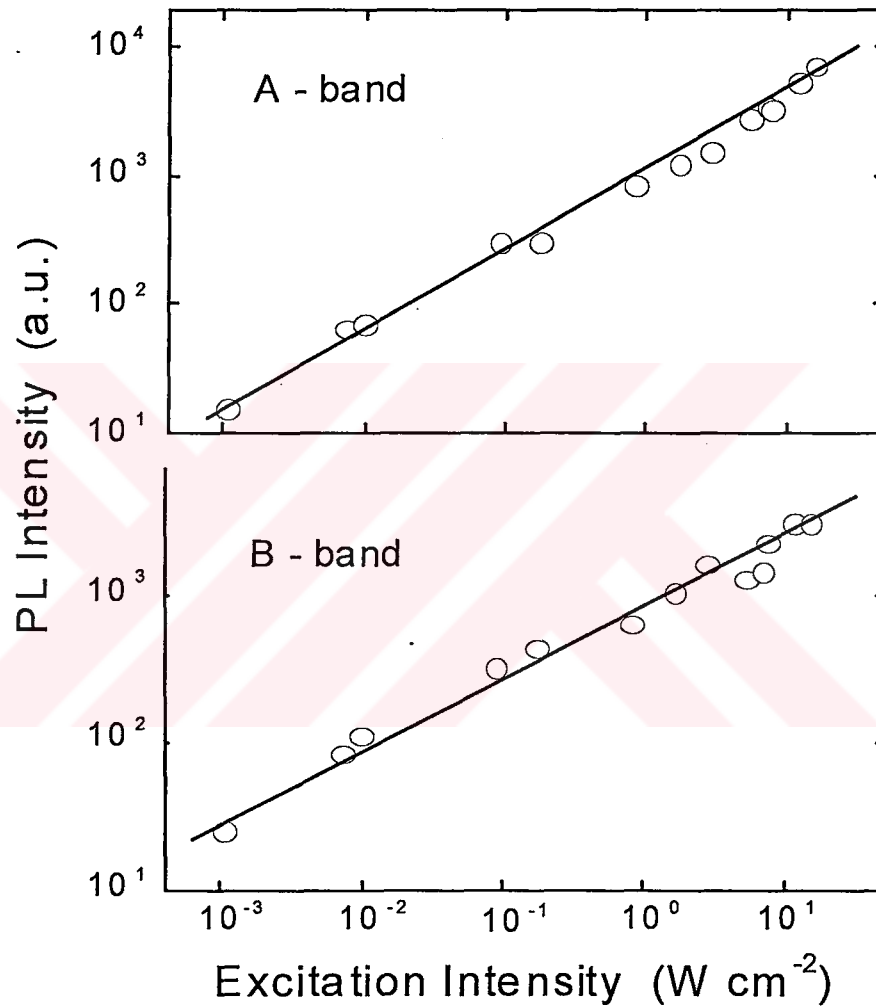


Fig. 4.11. Dependencies of the photoluminescence intensity at the A- and B-bands maximum versus excitation laser intensity at T = 15 K

The analysis of the observed PL spectra as a function of both the temperature and excitation laser intensity permits us to propose a possible scheme for the donor-acceptor levels located in the band gap of $\text{GaS}_{0.5}\text{Se}_{0.5}$. These donor-acceptor levels are involved in the radiative recombination of photoexcited carriers observed in $\text{GaS}_{0.5}\text{Se}_{0.5}$. Thus, two shallow donor levels d_1 and d_2 are located 0.029 and 0.040 eV below the bottom of of the conduction band, respectively (Fig. 4.12).

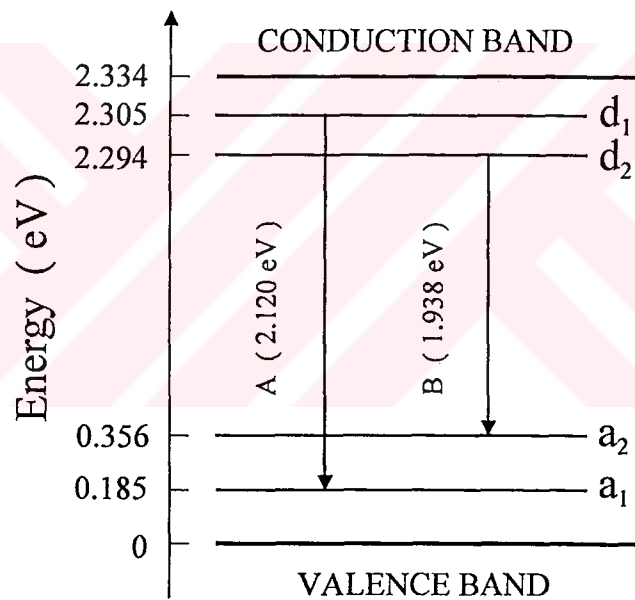


Fig. 4.12. Proposed energy band diagram for the observed deep level luminescence in $\text{GaS}_{0.5}\text{Se}_{0.5}$ at $T = 15\text{ K}$

Recalling the general expression for the emission energy of the donor-acceptor pair from Eqn. (2.6) [54] and neglecting the fourth term in the above equation which is a correction for Coulombic interaction between the pairs and is effective at short distances, we find the acceptor levels a_1 and a_2 above the top of the valence band at 0.185 and 0.356 eV, respectively.

As Eqn. (2.6) makes it clear, contribution from pairs with larger separation results in red shift of the peak energy of the observed band. This is the case for both bands. The smaller shift of the A-band upon temperature rise indicates that the distribution of the donor-acceptor pair separations involved in the recombination is restricted to narrower range of R values than those involved in B-band.

Sublinear PL intensity with excitation laser intensity is also consistent with donor-acceptor recombination [37]. Our analysis shows that the peak energy positions of the observed bands do not shift with increasing laser excitation intensity in line with the fact that the states involved in the recombination are indeed close pairs. If the donor-acceptor pair distances were heterogeneous in nature, then Eqn. (2.6) indicates that increasing the excitation laser intensity should show a blue shift of the peak energies of the PL bands which is clearly not observed.

4.3.3 Conclusions

In conclusion, we have measured the low temperature PL spectra of $\text{GaS}_{0.5}\text{Se}_{0.5}$ crystal grown by the Bridgman method as a function of temperature and excitation laser intensity. We have found two emission bands centered at 585 nm (2.120 eV, A-band) and 640 nm (1.938 eV, B-band) in the PL spectrum at 15 K. The onset of strong

quenching of the A-band is 50 K whereas it is 90 K for the B-band. Both temperature and excitation laser intensity dependencies of the PL spectra suggest that shallow donor and deep acceptor levels in the band gap of GaS_{0.5}Se_{0.5} can account for the observed emission. The fact that the peak energies do not show a blue shift upon increasing laser intensity indicate that both bands originate from closely spaced pairs. Smaller peak energy shift of the A-band with temperature suggests narrower range of pair separations. Since the samples are not intentionally doped, the donor and acceptor states are thought to originate from defects in the crystal.

4.4 Results and Discussion of the PL Experiment for GaSe crystal

4.4.1 Experimental Details

Single crystals of ϵ -GaSe were grown by the modified Bridgman method. The analysis of X-ray diffraction data showed that GaSe crystallizes in a hexagonal unit cell with lattice parameters $a = 0.3745$ and $c = 1.5921$ nm [46]. The samples were prepared by cleaving an ingot parallel to the crystal layer, which was perpendicular to the c -axis with typical sample dimensions of $4 \times 3 \times 0.7$ mm³. The studied samples were p -type as determined by the hot-probe method. "Spectra-Physics" He-Ne and an Ar ion lasers operating at wavelengths of 632.8, 514.5, and 488.0 nm were used as the excitation source. The PL was observed from the laser-illuminated face of the samples, in a direction close to the normal of the (001) plane. The PL spectra in the 635-750 nm wavelength range were analysed. A set of neutral-density filters was used to adjust the excitation laser intensity from 4.8×10^{-3} to 4.30 W cm⁻².

4.4.2 Results and Discussion

We first used the 488.0 and 514.5 nm wavelengths of the Ar ion laser to excite PL in GaSe. For both wavelengths, this results in intense near-band-edge emission due to recombination of direct and indirect free and bound excitons which are well characterized in GaSe. No other features have been observed beyond 635 nm. These results are in agreement with those previously obtained [56]. In fact, it has long been recognized that the observation of non-excitonic emission in GaSe requires low pumping power, high impurity content or very low temperatures [18]. Alternatively, longer excitation wavelengths can also be used to try to observe non-excitonic PL from GaSe [57]. In the present work, we concentrate on non-excitonic PL spectra obtained by excitation with 632.8 nm line of a He-Ne laser.

Fig. 4.13 shows typical non-excitonic PL spectra obtained from GaSe single crystals as measured in the 635-750 nm wavelength and 10-150 K temperature range at a constant excitation intensity of 4.30 W cm^{-2} . We observe two broad bands labelled as A- and B-bands. The A-band is lower in intensity while the intensity of the B-band dominates the spectrum. We deconvoluted the spectra with two Gaussian peaks using a least-squares approach and found that the PL bands are centred at 644 nm (1.925 eV) and 695 nm (1.784 eV) at 10 K. We note that both the PL intensity and the PL peak energy change as a function of increasing sample temperature. As the temperature is increased, the PL intensities of both bands decrease. All PL activity ceases to be observed at 150 K. The observed bands have Gaussian lineshapes and half-widths of 0.078 and 0.110 eV for the A- and B-bands, respectively. These features are typical of donor-acceptor pair recombination processes in semiconductors [58].

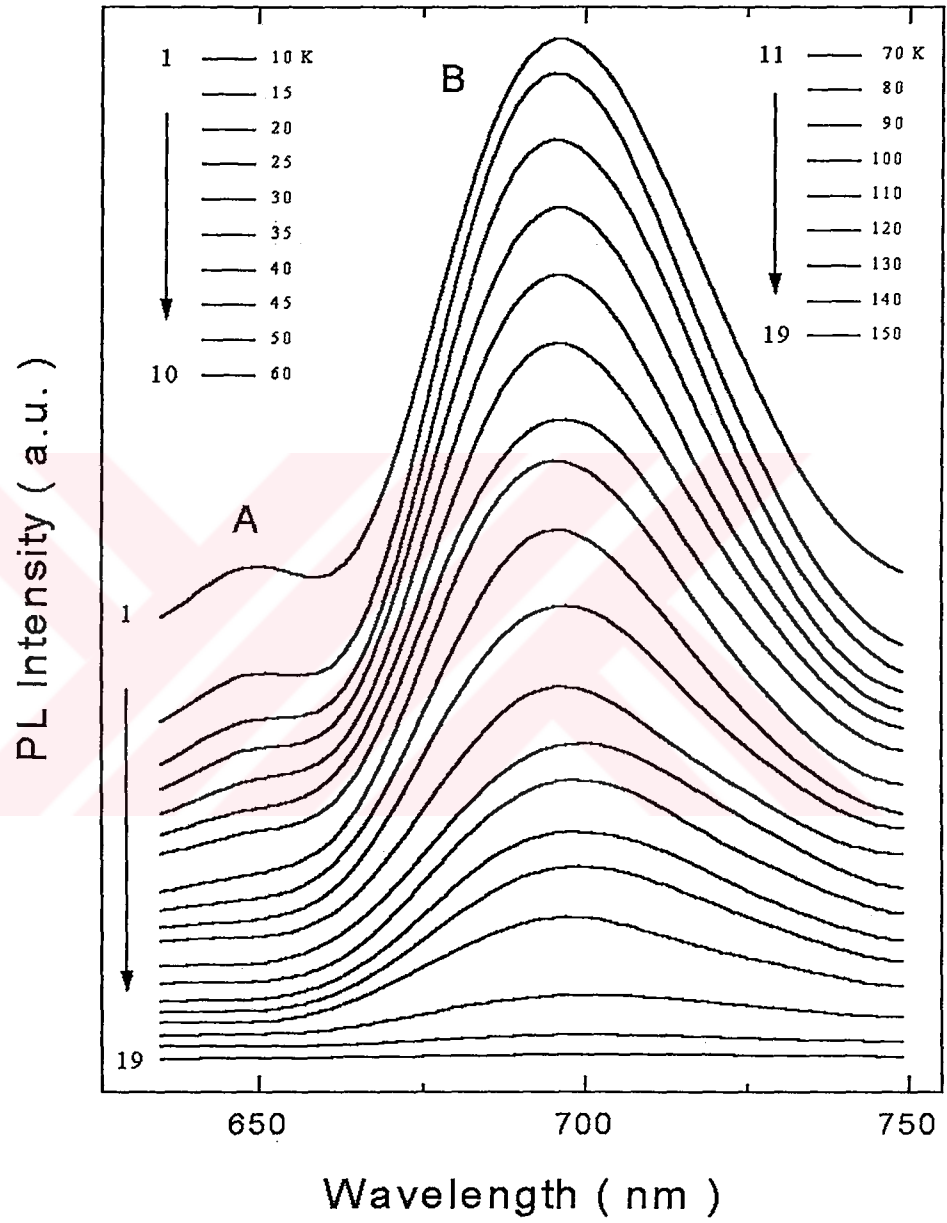


Fig. 4.13 PL spectra of undoped p-type GaSe as a function of temperature

From Fig. 4.13, it can be seen that the intensities of both bands decrease with temperature with the A-band quenching much faster than the B-band. The variations of the PL peak intensity of both bands with respect to temperature are plotted in Fig. 4.14. In the low-temperature range, the PL intensities of both bands decrease slowly. Above 35 K for the A-band and 90 K for the B-band, the rates of intensity decrease as both bands increase significantly due to thermal quenching processes. The activation energies for both bands have been obtained by fitting the high-temperature regions of the data to the Eqn. (4.1). The semilog plots of the peak intensity as a function of the reciprocal temperature give straight lines in the 35-70 K and 90-150 K regions for the A- and B-bands, respectively. The slopes of these lines give the activation energies as 0.014 eV for the A-band and 0.076 eV for the B-band. Since the as-grown GaSe is a *p*-type semiconductor, as confirmed by the measurement of the carrier type using the hot-probe method, we assume that the activation energies we obtained from Fig. 4.14 correspond to the activation energies of the acceptor levels. Similar assignments have been made for Ag- and Cu- doped *p*-GaSe [20, 15]. The activation energy of 0.076 eV obtained for the B-band can be compared with previous data obtained using various measurement techniques. From the temperature dependence of the dark conductivity in undoped *p*-GaSe, acceptor levels of 0.075 eV [59], 0.086 eV [60] and 0.070 eV [61] above the valence band were deduced. On the other hand, the temperature dependence of Hall coefficient has yielded a value of 0.066 eV [62]. The value of 0.076 eV obtained by us using the temperature dependence of the PL intensity is in fair agreement with this data. The activation energy of 0.014 eV that we obtained for the A-band corresponds to the ionization energy of a shallow level above the top of the valence band maximum and could not have been previously obtained since, to our knowledge, all measurements on GaSe were done and analysed at 80 K or higher.

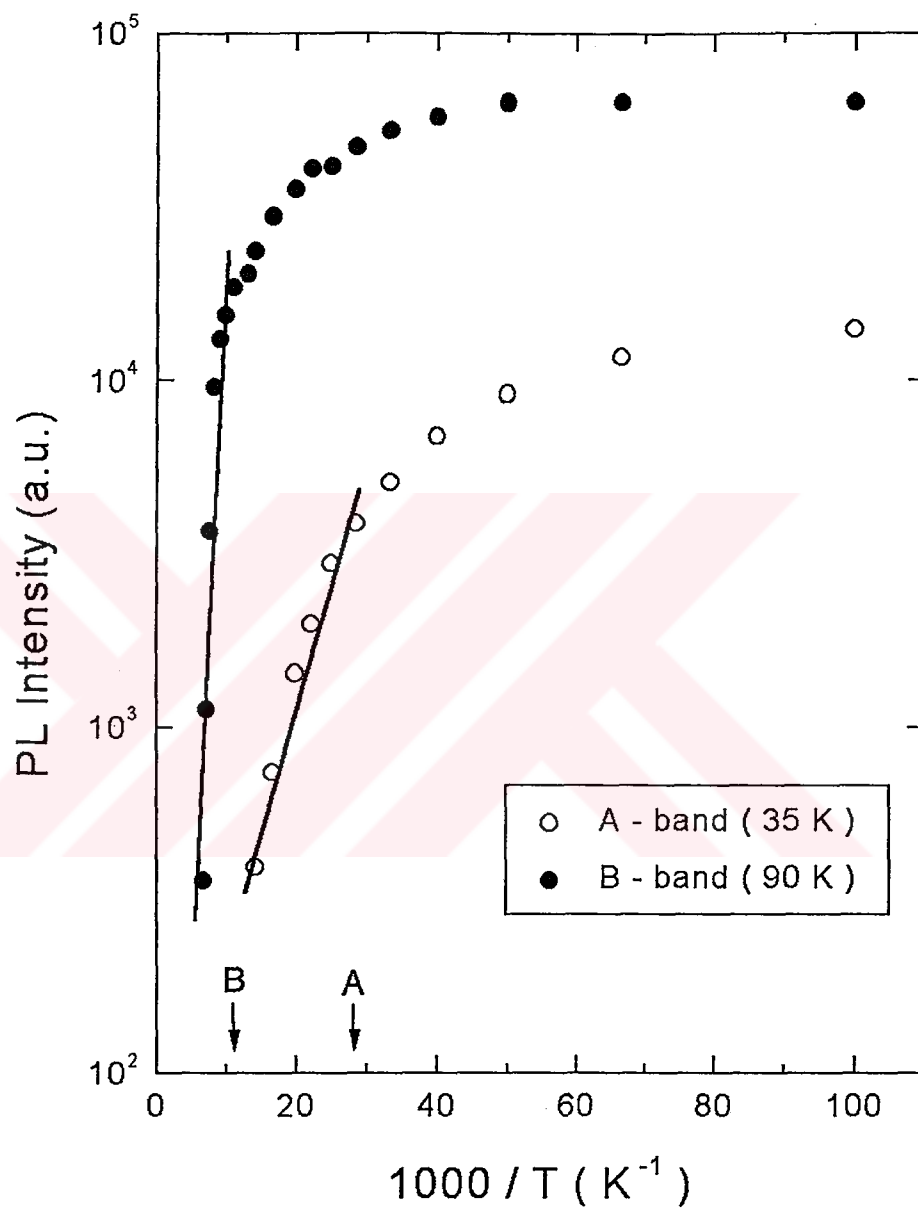


Fig. 4.14. Temperature dependences of GaSe PL intensity at the emission band maxima, the arrows at 35 and 90 K show the starting points of the intensive quenching of the A and B bands respectively

We have studied the temperature dependence of the peak energy of each band. PL emission obtained from the A- and B-bands quench totally above 70 and 150 K, respectively. The A-band shifts towards the red very slightly beyond 50 K. The B-band also shows a small red shift starting at 50 K and becoming larger beyond 100 K. Since for GaSe the rate of change of the band gap energy with temperature is negative, the observed red shifts are to be expected.

The behaviour of both bands as a function of excitation laser intensity has also been studied. We find that the peak energy of the A-band does not shift with increasing excitation laser intensity in contrast with the B-band. This may be due to a homogenous distribution of donor-acceptor pairs involved in the emission of the A-band. The dependence of the emission peak energy (E_p) of the B band at 10 K as a function of excitation laser energy intensity (I) is given in Fig. (4.15). Inspection of the data shows that the maximum of this band shifts towards higher energies from 1.770 to 1.784 eV ($\Delta E_p = 0.014$ eV) with increasing excitation laser intensity from 4.8×10^{-3} to 4.30 W cm^{-2} (i.e., 4.8 meV per decade of intensity of exciting radiation). This shift is relatively small because of the limited range of excitation laser intensity available from our He-Ne laser. The observed blue shift is characteristic of donor-acceptor pair recombination process. The magnitude of the observed blue shift is of the same order as in other binary and ternary semiconductor compounds such as ZnSe, GaP [63], InP [64], GaAs[65], TlGaSe₂ [66] and CuGaSe₂ [67], which are 3.2, 3.6, 2-10, 8.8, 6.0 and 6.8 meV per decade of exciting radiation intensity, respectively. In donor-acceptor pair recombination, photoexcited carriers trapped at donors and acceptors recombine radiatively. The energy of the emitted radiation due to recombination of carrier trapped at donor and acceptor sites

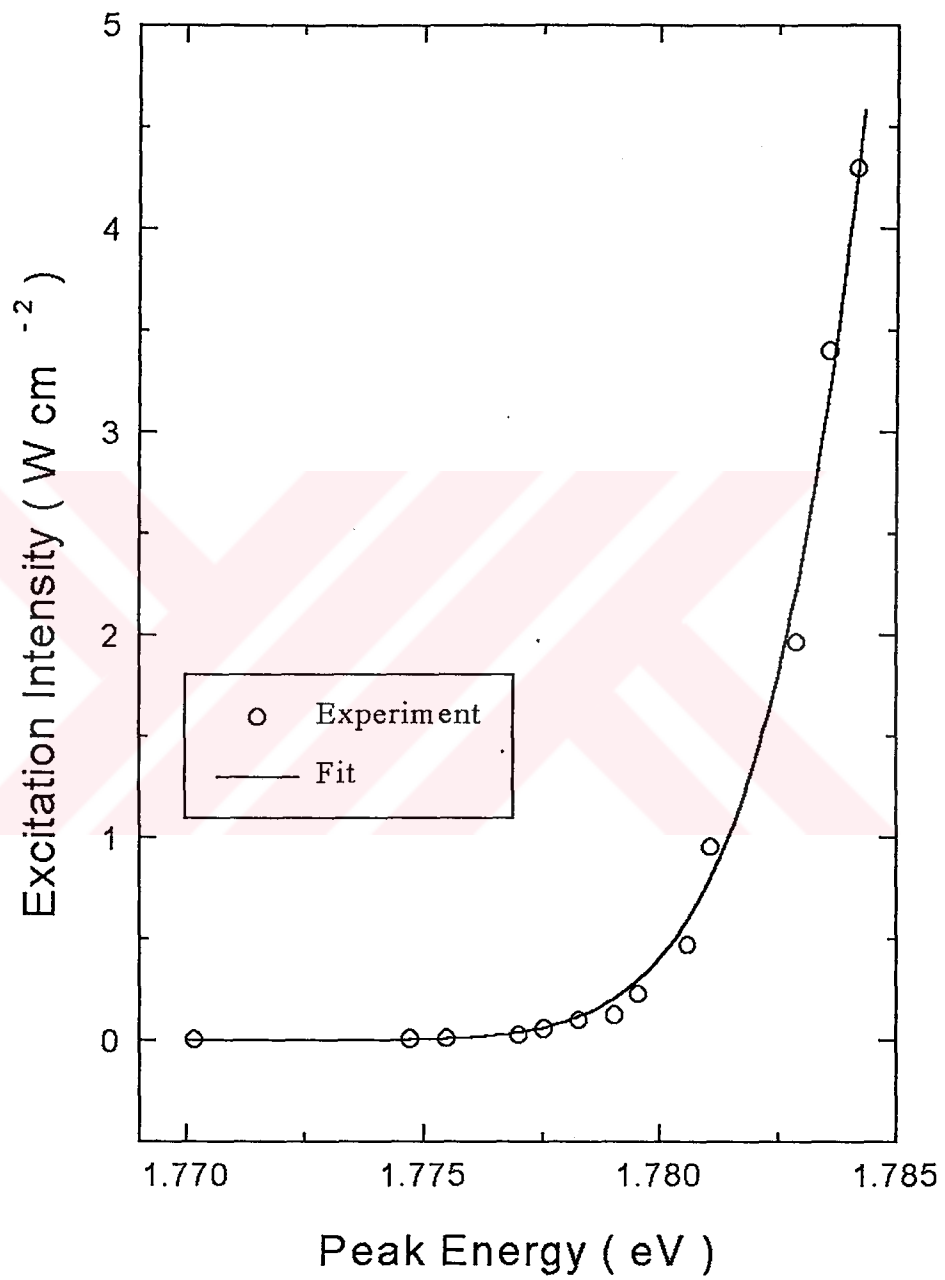


Fig. 4.15 Excitation laser intensity versus GaSe emission B-band peak energy at 10 K

is given by Eqn. (2.6). As can be seen from this equation, at low excitation laser intensities only distant pairs are excited [65]. At higher excitation intensities, closer pairs are also excited and contribute to the observed radiative intensity. On the other hand, Coulombic interaction between ionized sites is a function of the distance between the pairs and makes a positive contribution to the energy of the emitted photon. This contribution increases as the separation between the pairs decreases [31]. Furthermore, the radiative transition probabilities for different pair separations are not the same and decrease exponentially as a function of the pair distance [58]. We used Eqn. (2.37) [63] to fit the experimental data in Fig. 4.15. From a non-linear least-squares fit to the experimental data, the photon energies of an infinitely distant donor-acceptor pair and a close donor-acceptor pair separated by R_B are found to be $h\nu_\infty = E_\infty = 1.762$ eV and $h\nu_B = E_B = 1.832$ eV, respectively. These limiting photon energies are in good agreement with the band gap energy ($E_g = 2.102$ eV) and the observed values of the peak energy position (i.e., $E_\infty < 1.770$ eV $< E_p < 1.784$ eV $< E_B < E_g$) at 10 K.

We have also investigated the intensity variation of the maximum of the emission band versus the excitation laser intensity at $T = 10$ K (Fig. 4.16). The experimental data can be fitted by Eqn. (2.7). It was found that, the PL intensity increases sublinearly and yields values of $k = 0.97$ and $k = 0.95$ for the A- and B-bands, respectively. No saturation of the PL intensity was observed in the highest excitation laser intensity available to us. For an excitation laser energy larger than the band gap energy E_g of a semiconductor, the coefficient k is generally $1 < k < 2$ for free and bound exciton emission, and $k \leq 1$ for free-to-bound and donor-acceptor pair recombination [37]. Thus the obtained value of $k < 1$ for

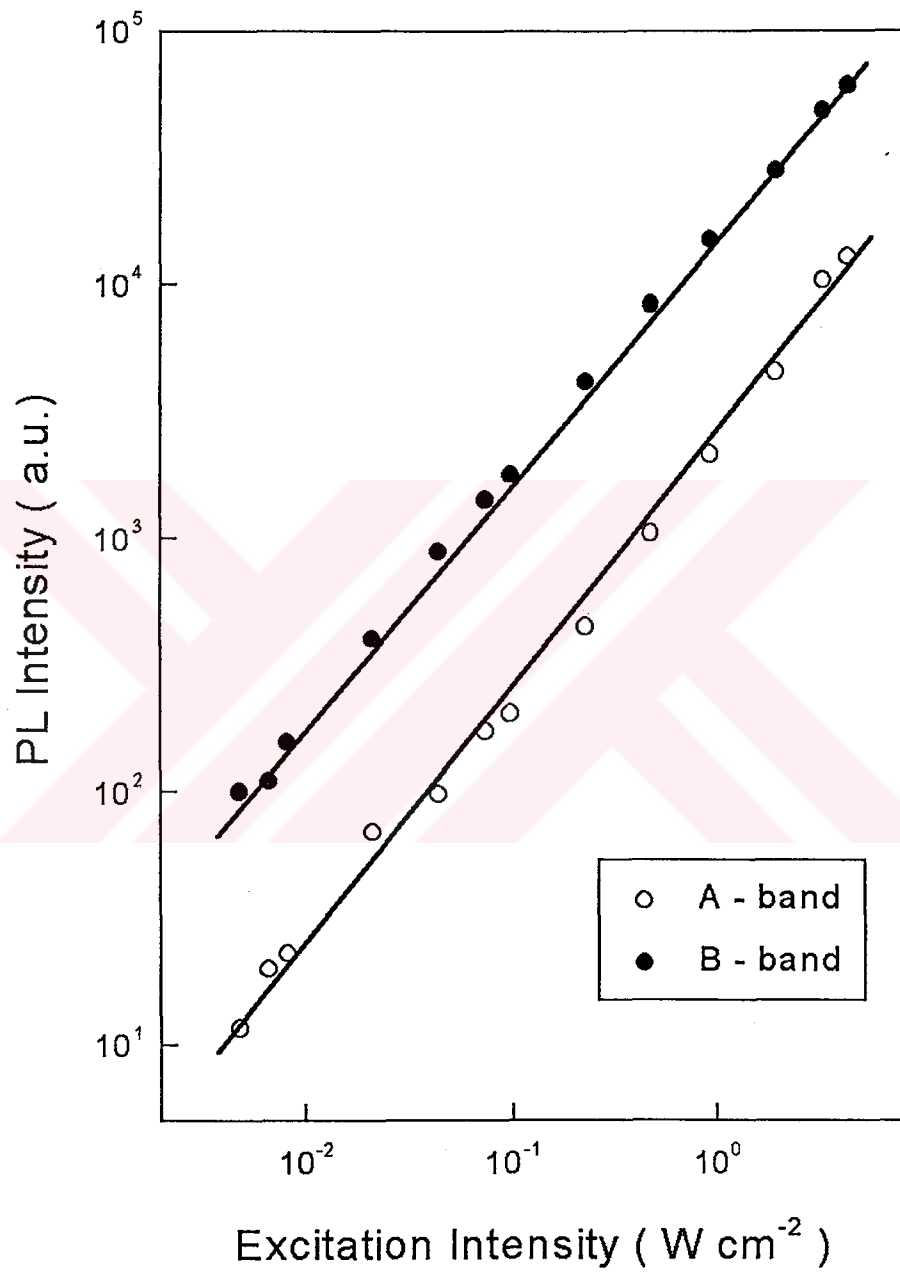


Fig. 4.16 Dependence of GaSe PL intensity at the emission band maxima vs. excitation laser intensity at 10K

both bands is further evidence that the observed emission is due to donor-acceptor pair recombination.

The analysis of the observed PL data as a function of temperature and excitation laser intensity allows us to propose a possible model for the donor-acceptor levels located in the forbidden gap of GaSe. These levels are involved in the radiative recombination of photoexcited carriers. In the model that we propose, the activation energies obtained from the temperature-dependent intensities of the A- and B-bands suggest the presence of two acceptor levels a_1 and a_2 which are located 0.014 eV and 0.076 eV above the valence band. On the other hand, using the general expression for the emission energy of the donor-acceptor pair and taking into account E_g and E_∞ , the sum of the activation energies of the donor (E_d) and acceptor levels (E_a) levels, involved in the emission band, can be estimated as:

$$E_a + E_d = E_g - E_\infty = (2.102 - 1.762) \text{ eV} = 0.340 \text{ eV} .$$

Considering that the acceptor level is located at 0.076 eV above the top of the valence band, this result suggests that the donor level involved in the emission of the B-band, d_2 , is located 0.264 eV below the bottom of the conduction band. For the A-band, the shallow acceptor level at 0.014 eV and the observed peak energy at 10 K (1.925 eV), results in a donor level, d_1 , which is located 0.163 eV below the bottom of the conduction band (Fig. 4.17). We propose that these moderately deep donor and shallow acceptor levels are associated with stacking faults or dislocations, which are easily produced in these materials due to weak van der Waals forces between the layers.

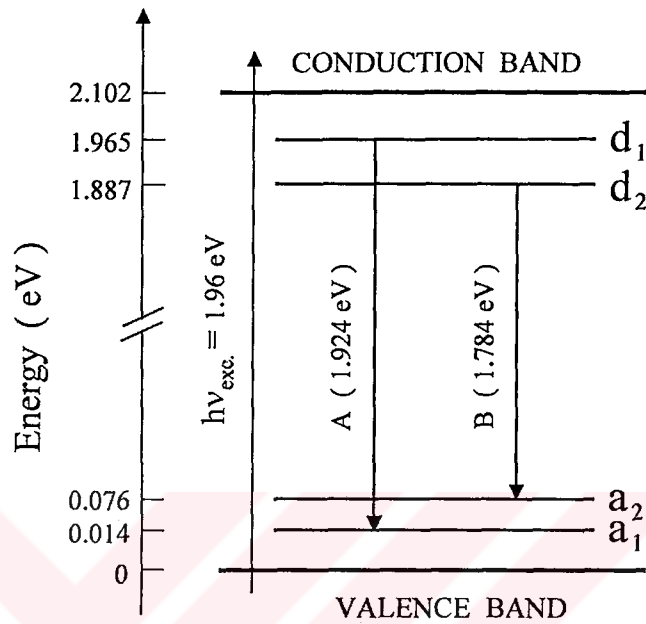


Fig. 4.17. Proposed energy band diagram for the observed deep level luminescence in GaSe at $T = 10$ K

Moderately deep donor levels were suggested in nominally undoped p -type GaSe layered crystals previously [15]. There, in addition to excitonic features, four weak bands centered at 645 (1.923), 662 (1.872), 700 (1.771), and 742 nm (1.672 eV) were observed at 80 K. Considering that $(dE_g/dT) = -0.47$ meV/K for GaSe, a blue shift of 33 meV should be expected for these lines at 10 K. Two of these lines (1.923 and 1.672 eV) were assigned to bound-to-free transitions from two donor levels to the valence band. The donor levels were located 0.170 and 0.420 eV below the bottom of

the conduction band. The donor level located at 0.170 eV below the conduction band agrees closely with our finding of a donor level at 0.163 eV below the conduction band. The other two transitions were thought to be due to donor-acceptor pair transitions from the first donor level to acceptor levels at 0.051 eV and 0.152 eV above the valence band maximum. In a later study [16] only two bands at 1.88 and 1.62 eV were observed at 80 K from nominally undoped *p*-GaSe beyond 635 nm. No activation energies of impurity levels involved in the emission were obtained from the temperature dependence of emitted intensities. In contrast with their earlier work, they assigned the high energy band to a transition from a shallow donor ($E_D = 0.006$ eV) to an acceptor level ($E_A = 0.20$ eV) and the low energy band to recombination of free electrons with deep neutral acceptors ($E_A = 0.44$ eV), using published values in the literature for donor and acceptor level activation energies obtained from electrical measurements. While the number of bands and the approximate spectral location of these bands that we observe is the same as those observed in their work, our conclusions and, except for the donor level at 0.163 eV, the initial and final states that are involved in these transitions are different. This may be due to the possibility of several donor and acceptor states, both deep and shallow, in undoped GaSe. The presence of any number of these states in a given GaSe crystal may depend on the details of the growth conditions of each crystal.

4.4.3 Conclusions

Non-excitonic PL spectra of undoped GaSe have been studied as a function of temperature and excitation laser intensity. Two broad bands at 644 and 695 nm were observed at 10 K. Considering the *p*-type behaviour of undoped GaSe, and the

activation energies obtained from the temperature dependence of the emitted intensities, we deduce two shallow acceptor levels at 0.014 and 0.076 eV above the top of the valence band maximum. From the peak energy positions of the bands, we infer the existence of two moderately deep donor levels at 0.163 and 0.264 eV below the bottom of the conduction band. We therefore propose that the bands that we observe are due to carrier recombination through neutral donor-acceptor pairs.



CHAPTER 5

CONCLUSIONS

A^{III}B^{VI}-type layered semiconductors attract much interest due to possible optoelectronic applications from ultraviolet to the infrared. For the most part, optoelectronic properties of these materials are dominated by defects of various types and the interactions between them. In spite of the significant experimental and theoretical efforts devoted to the study of these materials, both experimental data and the overall theoretical understanding of them lacks a coherent and complete framework. In fact, even in binary compounds, little work has been done both experimentally and theoretically. Most of the work on layered semiconductors has concentrated on the near band edge emission of these materials. Only a little amount of data exists on shallow and deep PL bands with emission energies below the band gaps of these semiconductors. In this work, we investigated low temperature photoluminescence properties of GaS_xSe_{1-x} mixed crystals for the values of $x = 1, 0.5$ and 0 . From the temperature dependence and laser excitation intensity dependencies of photoluminescence spectra, we got several results, as follows.

For $x = 1$ (GaS), photoluminescence spectra were studied as a function of temperature and excitation laser intensity. At 9 K, three PL bands at 2.22 eV (A-band), 2.02 eV (B-band), and 1.59 eV (C-band) have been observed. Both the excitation intensity and temperature dependencies of the bands suggest that nearest neighbor pairs

are responsible for the emissions. Deep acceptor and shallow donor levels in the band gap of GaS account for the observed emission for A- and B-bands. The peculiar behavior of the C-band is understood within the framework of a proposed configuration coordinate model. The changes in the FWHM of the C-band as a function of temperature imply that there may be two excited states. As the samples are not intentionally doped, donor and acceptor states are thought to originate from point defects.

For $x = 0.5$ ($\text{GaS}_{0.5}\text{Se}_{0.5}$), photoluminescence spectra were investigated as a function of temperature and excitation laser intensity. We have observed two emission bands centered at 585 nm (2.120 eV, A-band) and 640 nm (1.938 eV, B-band) in the PL spectrum at 15 K. The onset of strong quenching of the A-band is 50 K whereas it is 90 K for the B-band. Both temperature and excitation laser intensity dependencies of the PL spectra suggest that shallow donor and deep acceptor levels in the band gap of $\text{GaS}_{0.5}\text{Se}_{0.5}$ can account for the observed emission. The fact that the peak energies do not show a blue shift upon increasing laser intensity indicate that both bands originate from closely spaced pairs. Smaller peak energy shift of the A-band with temperature suggests narrower range of pair separations. Since the samples are not intentionally doped, the donor and acceptor states are thought to originate from defects in the crystal.

For $x = 0$ (GaSe), non-excitonic photoluminescence spectra were studied as a function of temperature and excitation laser intensity. Two broad A- and B-bands at 644 and 695 nm were observed at 10 K. Experiments revealed that the peak energy of the A-band does not shift with increasing excitation laser intensity in contrast to that of B-band. These behaviours are attributed to the homogenous and non-homogenous distributions of donor-acceptor pairs involved in the emission of A-

and B-bands, respectively. Considering the *p*-type behaviour of undoped GaSe, and the activation energies obtained from the temperature dependence of the emitted intensities, we deduce two shallow acceptor levels at 0.014 and 0.076 eV above the top of the valence band maximum. From the peak energy positions of the bands, we infer the existence of two moderately deep donor levels at 0.163 and 0.264 eV below the bottom of the conduction band. We therefore propose that the bands that we observe are due to carrier recombination through neutral donor-acceptor pairs.

The results of photoluminescence experiments done on GaS_xSe_{1-x} mixed crystals for the values of $x = 1, 0.5$ and 0 revealed the underlying recombination mechanisms for each crystal, especially in the low temperature region which has not been investigated before. The study of the photoluminescence spectra as a function of temperature and excitation laser intensity demonstrated that neutral donor-acceptor pairs were responsible for the emission bands. Energy band diagram for donor-acceptor pair transitions is drawn for crystals studied.

REFERENCES

- [1] Klaus D. Mielenz,
Optical radiation measurements: Measurement of Photoluminescence,
p. iv, Academic Press, New York (1982).
- [2] K. A. Yee and A. Albright, *J. Am. Chem. Soc.* **113**, 6474 (1991).
- [3] A. G. Kyazm-zade, R. N. Mekhtieva, and A. A. Akhmedov,
Sov. Phys. Semicond. **25**, 840 (1992).
- [4] E. Aulich, J. L. Brebner, and E. Mooser, *Phys. Status Solidi* **31**, 129 (1969).
- [5] A. Mercier, and J. P. Voitchovsky, *J. Phys. Chem. Solids* **36**, 1411 (1975).
- [6] C. Manfredotti, A. Rizzo, A. Bufo, V. L. Cardetta, *Phys. Stat. Solidi (a)* **30**,
375 (1975).
- [7] N. M. Gasanly, *D. Sci. Thesis. Baku State University, Azerbaijan*, (1986).
- [8] G. Akhundov, I. G. Aksyanov, and G. M. Gasumov, *Sov. Phys. Semicond.* **3**,
767 (1969).
- [9] M. I. Karaman and V. P. Mushinskii, *Sov. Phys. Semicond.* **4**, 662 (1970).
- [10] A. Cingolani, A. Minafra, P. Tantalo, and C. Paorici, *Phys. Status Solidi A* **4**,
K 83 (1971).
- [11] T. Aono, K. Kase, and A. Kinoshita, *J. Appl. Phys.* **74**, 2812 (1993).
- [12] A. Mercier, E. Mooser, and J. P. Voitchovsky, *J. Lumin.* **7**, 241 (1973).
- [13] M. I. Karaman and V. P. Mushinskii, *Sov. Phys. Semicond.* **4**, 464 (1970).
- [14] V. Capozzi, *Phys. Rev. B* **23**, 836 (1981).
- [15] V. Capozzi, *Phys. Rev. B* **28**, 4620 (1983).
- [16] V. Capozzi, and M. Montagna, *Phys. Rev. B* **40**, 3182 (1989).

- [17] B. Tagiev, G. M. Niftiev, and F. S. Aidaev, *Phys. Stat. Sol. (b)* **128**, K 65 (1985).
- [18] J. P. Voitchovsky, and A. Mercier, *Nuovo Cim. B* **22**, 273 (1974).
- [19] S. Shigetomi, T. Ikari, and H. Nakashima, *J. Appl. Phys.* **69**, 7976 (1991).
- [20] S. Shigetomi, T. Ikari, and H. Nakashima, *Phys. Stat. Sol. (a)* **160**, 159 (1997).
- [21] B. Tagiev, G. M. Niftiev, and S. A. Abushov, *Phys. Stat. Sol. (b)* **121**, K 195 (1984).
- [22] S. Shigetomi, T. Ikari, and H. Nakashima, *J. Appl. Phys.* **74**, 4125 (1997).
- [23] Ph., Schmid, J. P. Voithchovsky, and A. Mercier, *Phys. Stat. Sol. (a)* **21**, 443 (1974).
- [24] V. Riede, F. Levy, H. Neumann, H. Sobotta, *Solid State Commun.* **34**, 229 (1980).
- [25] N. M. Gasanly, A. F. Goncharov, N. N. Melnik, A. S. Ragimov, *Phys. Stat. Sol. (b)* **120**, 137 (1983).
- [26] M. Heyek, O. Brafman, R. M. A. Lieth, *Phys. Rev. B* **8**, 2772 (1973).
- [27] A. Mercier, and J. P. Voithchovsky, *Solid. Stat. Commun.* **14**, 757 (1974).
- [28] Yu. P. Gnatenko, I. A. Farina, R. V. Gamernik, V. S. Blashkiv and A. S. Krochuk, *Semiconductors* **30**, 1027 (1996).
- [29] A. G. Milnes, *Deep Impurities in Semiconductors*, p. vii, John Wiley and Sons, New York (1973).
- [30] H. Serizawa, Y. Sasaki, and Y. Nishina, *Jour. of the Phys. Soc. of Japan* **48 (2)**, 490 (1980).
- [31] P. Y. Yu., M. Cardona, *Fundamentals of Semiconductors*, p. 348, Springer, Berlin (1995)
- [32] P. J. Dean, *Prog. Cryst. Growth Charact.* **5**, 89 (1982).
- [33] T. Taguchi, J. Shirafuji and Y. Inuishi, *Phys. Status Solidi B* **68**, 727 (1975).
- [34] D. E. Cooper, J. Bajaj and P. R. Newmann, *J. Cryst. Growth* **86**, 544 (1988).
- [35] Z. C. Feng, A. Mascarenhas and W. J. Choyke, *J. Lumin.* **35**, 329 (1986).
- [36] Q. Kim and D. W. Langer, *Phys. Status Solidi B* **122**, 263 (1984).

- [37] T. Schmidt, K. Lischka and W. Zulehner, *Phys. Rev. B* **45**, 8989 (1992).
- [38] M. I Nathan and T. N. Morgan, *Physics of Quantum Electronics*, p. 478, McGraw-Hill (1966).
- [39] D. G. Thomas, M. Gershenson and F. A. Trumbore, *Phys. Rev.* **133**, A 269 (1964).
- [40] K. Maeda, *J. Phys. Chem Solids* **26**, 595 (1965).
- [41] P. J. Dean and J. L. Merz, *Phys. Rev.* **178**, 1310 (1969).
- [42] E. Zacks, A. Halperin, *Phys. Rev. B* **6**, 3072 (1972).
- [43] D. G. Thomas, J. J. Hopfield and W. M. Augustiniak, *Phys. Rev.* **140**, A202 (1965).
- [44] P. J. Dean and L. Patrick, *Phys. Rev. B* **2**, 1888 (1970).
- [45] M. Lax, *J. Phys. Chem Solids* **8**, 66 (1959).
- [46] A. Kuhn, A. Chevy and R. Chevalier, *Phys. Stat. Sol.* **36**, 181 (1976).
- [47] C.C. Klick and J.H.Schulman, *Solid State Physics*, Vol. 5, p. 110, Academic Press (1957).
- [48] A.Aydinli, N.M. Gasanly, I. Yilmaz, and A. Serpenguzel, *Semicond. Sci. Technol.* **14**, 599 (1999).
- [49] J. Krustok, J.H. Schon, H. Collan, M. Yakushev, J. Mudasson, and E. Bucher, *J. Appl. Phys.* **86**, 364 (1999).
- [50] F. Williams, *Phys. Status Solidi* **25**, 493 (1968).
- [51] J. H. Schon, O. Schenker, H. Riazi-Nejad, K. Friemelt, Ch. Kloc, and E. Bucher, *Phys. Status Solidi A* **161**, 301 (1997).
- [52] A. Segura and A. Chevy, *Phys. Rev. B* **49**, 4601 (1994).
- [53] A. Gauthier, A. Polian, J.M. Besson, and A. Chevy, *Phys. Rev. B* **40**, 3837 (1989).
- [54] P. Y.Yu., M. Cardona, *Fundamentals of Semiconductors*, p. 344, Springer, Berlin (1995).
- [55] A. Aydinli, N.M. Gasanly, and K. Goksen, *J. Appl. Phys.* **88**, 7144 (2000).

- [56] S. Shigetomi, T. Ikari, and H. Nishimura, *J. Appl. Phys.* **69**, 7936 (1991).
- [57] Y. P. Gnatenko, Y. I. Zhirko, and Z. D. Kovalyuk, *Phys. Stat. Sol. B* **161**, 427 (1990).
- [58] J.P. Leyris, J.P. Aicardi, and S. Soule, *J. Lumin.* **28**, 65 (1983).
- [59] C. Tatsuyama, C. Hamaguchi, H. Tomitha, and J. Nakai, *Jpn. J. appl. Phys.* **10**, 1698 (1971).
- [60] C. Manfredotti, A. Rizzo, C. De Blasi, S. Galassini, and L. Rugierro, *J. appl. Phys.*, **46**, 4531 (1975).
- [61] F. I. Ismailov, G. A. Akhundov, and O.R. Vernich, *Phys. Stat. Sol.* **17**, K237 (1966).
- [62] C. Manfredotti, A.M. Mancini, R. Murri, A. Rizzo, and L. Vasanelli, *Nuovo Cim. B* **39**, 257 (1977).
- [63] E. Zacks, and A. Halperin, *Phys Rev. B* **6**, 3072 (1972).
- [64] E. A. Montie, and G. J. van Gorp, *J. Appl. Phys.* **66**, 5549 (1989).
- [65] J. I. Pankove, *Optical Processes in Semiconductors*, p. 150, Prentice Hall, New Jersey (1971).
- [66] N.M. Gasanly, A. Serpenguzel, A. Aydinli, and S.M.A. Baten, *J. Lumin.* **86**, 39 (2000).
- [67] A. Poure, J.P. Leyris, and J.P. Aicardi, *J. Phys. C: Solid State Phys.* **14**, 521 (1981).